LANGMUIR



Interface Components: Nanoparticles, Colloids, Emulsions, Surfactants, Proteins, Polymers

# Conducting polymer-TiO2 hybrid materials: application in the removal of nitrates from water

Juan José Villora-Picó, Víctor Belda-Alcázar, M. Jesús García-Fernández, Elena Serrano, Antonio Sepúlveda-Escribano, and M. Mercedes Pastor-Blas

*Langmuir*, **Just Accepted Manuscript** • DOI: 10.1021/acs.langmuir.9b00174 • Publication Date (Web): 15 Apr 2019



ACS Publications

is published by the American Chemical Society. 1155 Sixteenth Street N.W., Washington, DC 20036

# Conducting polymer-$TiO_2$ hybrid materials: application in the removal of nitrates from water

*Juan José Villora-Picó[(a)], Víctor Belda-Alcázar[(a)], M. Jesús García-Fernández[(a)], Elena Serrano[(b)], A. Sepúlveda-Escribano [(a)], M. Mercedes Pastor-Blas[(a)]**

(a) Laboratorio de Materiales Avanzados, Departamento de Química Inorgánica – Instituto Universitario de Materiales de Alicante, Universidad de Alicante, Apartado 99, E-03080 Alicante. SPAIN.

(b) Laboratorio de Nanotecnología Molecular, Departamento de Química, Universidad de Alicante, Apartado 99, E-03080 Alicante. SPAIN.

KEYWORDS. Titania-polymer hybrids; nitrate reduction; platinum nanoparticles; plasma treatment.

.

ABSTRACT. Materials able to produce the reduction of nitrate from water without the need of a metal catalyst and avoiding the use of gaseous hydrogen have been developed by combining the synergistic properties of titania and two conducting polymers. Polymerization of aniline and pyrrol on titanium dioxide in the presence of two different oxidants/dopants (iron trichloride or potassium persulfate) has been evaluated. The resulting hybrid materials have good thermal stability imparted by the titania counterpart, and a considerable conductivity provided by the conducting polymers. The capability of the hybrid materials of reducing aqueous nitrate has been assessed and compared to the catalytic hydrogenation of nitrate using a platinum catalyst supported on these hybrid synthesized materials. The mechanism of nitrate abatement implies adsorption of nitrate on the polymer by ion exchange with the dopant anion, followed by the reduction of nitrate. The electrons transfer

from titania to the conducting polymer in the hybrid material favors the reductive ability of the polymer, in such a way that nitrate is selectively reduced with a very low production of undesirable side products. The obtained results show that the activity and selectivity of the catalytic reduction of nitrate with dihydrogen in the presence of a platinum catalyst supported on the hybrid materials is considerably lower than those of the metal-free nanocomposites.

## INTRODUCTION

The increasing use of nitrogenous fertilizers is responsible for nitrogen species permeation through the soil layers and contamination of groundwater. Methemoglobinemia and cancer are diseases produced by the human consumption of water exceeding the maximum permitted level of nitrate of 50 $mg \cdot L^{-1}$ [1,2]. Nitrates may be reduced to nitrites within the human body. Nitrite combine with hemoglobin, which contains the ferrous ($Fe^{2+}$) ion, to form methemoglobin, which contains the ferric ($Fe^{3+}$) form of iron. The increased affinity for oxygen of methemoglobin leads to an overall reduced ability of the red blood cell to release oxygen to tissues. When methemoglobin concentration is too high in red blood cells, tissue hypoxia may occur. This disease, known as the blue baby syndrome, is fatal to the new born. Physicochemical, biological and catalytic processes are available for removing nitrates from water[3]. Physicochemical methods as ion-exchange, reverse osmosis and electro-dialysis remove nitrates from drinking water but concentrate them elsewhere, with the subsequent disposal problem of the generated nitrate waste brine; biological denitrification transforms nitrates into molecular nitrogen, but is difficult to operate and may become another source of contamination of water with bacteria.

Catalytic reduction of nitrate species to form nitrogen has been considered as an alternative technology for nitrate abatement. Nitrate reduction is generally carried out with hydrogen ($H_2$) in the presence of metal catalysts. Monometallic systems as Pt or Pd, and also bimetallic systems combining a metal catalyst (Pd, Pt) and a promoter (Cu, In, Sn) have been successfully[4] dispersed on different supports showing a relatively high surface area as activated carbons,[5] carbon nanotubes,[6] zeolites[7] and metal oxides [8,9,18,10–17] as well as cation exchange resins.[19] It has been demonstrated that the reaction progresses through intermediate

nitrite ($NO_2^-$) and nitrogen and ammonium are the principal products of the catalytic reduction of nitrate ($NO_3^-$) with dyhidrogen ($H_2$). Numerous investigations and discussions have been performed to clarify the reaction intermediates.[20–22] They have demonstrated that nitrite ions are reduced on the surface of the noble metal to adsorbed NO as the key intermediate in the generation of nitrogen ($N_2$) and ammonium ($NH_4^+$). Two different pathways for the reduction of NO to $NH_4^+$ have been proposed: NO dissociation and NO hydrogenation. Different successive intermediates are produced, i.e. adsorbed NH, $NH_2$, and $NH_3$ when the reaction progresses through NO dissociation and adsorbed HNO, $H_2NO$, $H_2NOH$, $NH_2$ and $NH_3$ when the reaction progresses trough NO hydrogenation.

It had been widely accepted that the reduction of nitrate requires the promotion of the noble metal by addition of a second metal.[4,23] The role of the noble metal is to activate hydrogen, which reduces the promoter metal, completing the catalytic cycle. This is the accepted mechanism for non-reducible supports. However, nitrate reduction has been successfully achieved with monometallic catalysts on partially reduced supports as $TiO_2$. In this case, the reduction of nitrates is promoted by sites of the partially reduced support.[24–26] The most likely mechanism for nitrate uptake in the presence of water is via displacement of surface hydroxyl groups in $TiO_2$.[14] The nitrate anions are adsorbed on exposed Lewis acid sites of $TiO_2$ (unsaturated surface $Ti^{3+}$ sites) produced as a consequence of the removal of surface oxygen during the reduction process. The reduction of the coordination number of titanium cations leads to the presence of oxygen vacancies and a consequent positive charging of the surface, which results in the creation of favorable sites for the adsorption of anionic species as nitrate anions. These sites are expected to be located at the vicinity of the noble metal (usually Pd or Pt). The electrons, associated with the reduction process, may be

located on the $Ti^{3+}$ sites. In the literature there is evidence that the electrons are transferred from the support to the metal; however it has also been reported that nitrate can be reduced by electron enriched titania species (probably $Ti_4O_7$ formed by hydrogen spillover), producing nitrites as a stepwise reaction, which are subsequently hydrogenated leading to molecular nitrogen or ammonium.[18] Evidence of the existence of $Ti_4O_7$ species have been provided in $TiO_2$ after reduction at ~500ºC. The presence of the noble metal influences the state of the titania support prior to nitrate adsorption, so reduction of nitrates relies on a strong metal-support interaction and it is also dependent on the metal supported on $TiO_2$.

In previous works[27,28] nitrate abatement has been accomplished using a metal catalyst supported on conducting polymers with a very low surface area as polypyrrole. It was demonstrated that –NH- groups in polypyrrole are anchoring sites for the metal precursor, which results in a high dispersion of the active metal. The platinum nanoparticles supported on polypyrrole, obtained after treatment with an argon plasma, selectively catalyzed the reaction of reduction of nitrates in water with dyhydrogen towards nitrogen. However, the use of gaseous hydrogen[29] as a reactive agent to reduce nitrates represents a safety hazard. Besides, the polymeric support has a limited thermal stability, which limits its application for other reactions at temperatures above 150 ºC.

The goal of this investigation is to develop materials that are able to produce the green and safe reduction of nitrate from water without the need of a metal catalyst and avoiding the risks associated with the use of gaseous hydrogen. For that purpose, ceramic/polymeric

hybrid materials have been synthesized by the oxidative chemical polymerization of aniline or pyrrole onto $TiO_2$ to produce hybrid materials with synergistic properties.

It is well known the tendency of $TiO_2$ to oxygen deficiency,[30–37] which is evidenced by the creation of oxygen vacancies and the reduction of some $Ti^{4+}$ to $Ti^{3+}$, which imparts its capability of electron donor; consequently, it is widely considered to be a strongly n-type semiconductor.[38] However, some studies have demonstrated the ability of $TiO_2$ to act either as n or p-type semiconductor. The latter occurs under strongly oxidizing conditions, as a result of formation of titanium vacancies [39–41] or by doping $TiO_2$ with a suitable acceptor.[42–44]

The polymeric part of the hybrid material prepared in this work is a conducting polymer (polypyrrol or polyaniline) synthesized onto the $TiO_2$ particles by oxidative chemical oxidation of their monomers. If the fully oxidized form is obtained, the conducting polymer would behave as a p-type semiconductor. However, conducting polymers can switch between different redox states. Therefore, depending of the degree of oxidation achieved during the oxidative polymerization, the conducting polymer may act either as a source or a drain of electrons, depending on the process in which it is involved.[45] Consequently, upon polymerization of pyrrole or aniline onto titanium dioxide, electron transfer would be possible in both directions due to the capability of both materials to accept and donate electrons.

It must also be taken into consideration that during the oxidative chemical polymerization of aniline or pyrrole, the polymer is simultaneously doped with the anions provided by the oxidant. These counterions in the reaction medium are incorporated into the growing polymeric chains to maintain the electrical neutrality of the polymer system,[46] and

might be easily exchanged by nitrate ions ($NO_3^-$) present in contaminated water. Therefore, different dopants introduced by different oxidants, as $FeCl_3$ or $K_2S_2O_8$, are expected to have different performances in the adsorption of nitrates.

A synergistic behaviour between the conductive polymers and the titania is expected. The ion exchange properties of the polymer in these hybrid materials and the redox properties of both the polymer and the titanium dioxide, would make these materials suitable for application in the abatement of nitrate from water, not as support of the active metal catalyst, but participating themselves in the reaction of nitrate reduction. This would lead to a metal-free method of abatement of nitrates from water without the risks associated with the use of gaseous hydrogen. The mechanism of nitrate abatement and the role of both, titania and polymer counterparts, in the hybrid materials will be discussed.

## EXPERIMENTAL

### *Hybrid materials preparation*

$TiO_2$/PANI and $TiO_2$/PPy hybrid materials were prepared by oxidative chemical polymerization of aniline and pyrrol on commercial $TiO_2$ (Degussa P-25, 80% anatase, 20% rutile,[47]) previously calcined at 500 ºC for 5 h in order to obtain mainly the anatase phase. Different $TiO_2$:monomer ratios (60:40, 50:50 and 40:20) were used.

For the synthesis of $TiO_2$/PPy two different oxidants, $FeCl_3 \cdot 6H_2O$ and $K_2S_2O_8$, were used. The oxidant was added in excess so the oxidant/pyrrole molar ratio was 2.33.[48] 2 mL of pyrrole ($C_4H_5N$) were added dropwise to calcined $TiO_2$. The oxidant solution was prepared

by dissolving 18 g of oxidant ($FeCl_3 \cdot 6H_2O$ or $K_2S_2O_8$) in 400 ml of ultrapure water. This ferric chloride solution showed an orange color whereas the potassium persulfate solution was colorless. However, as soon as the pyrrole mixed with the oxidant solution it turned to its characteristic black colour, this indicating the formation of polypyrrole (PPy) in its doped form onto $TiO_2$. The solution was stirred for 6 h at room temperature. Then, the precipitated $TiO_2$/PPy powder was filtered, washed with distilled water and dried at 80 ºC for 12 h.

For the synthesis of $TiO_2$/PANI, only potassium persulfate ($K_2S_2O_8$) was used as oxidant, as a very low yield was obtained with iron chloride. The oxidant/aniline molar ratio was 1.25.[49] 2 mL of aniline ($C_6H_5NH_2$) were added drop wise under magnetic stirring to the required quantity of calcined $TiO_2$. Synthesis of polyaniline requires an acidic medium so 7.4 g of $K_2S_2O_8$ were dissolved in 150 ml of HCl (0.2M), and this solution was added to the $TiO_2$/aniline suspension. Polymerization of aniline took place as soon as the oxidant was in contact with aniline. Solution showed a blue color, characteristic of emeraldine base, which turned within seconds into dark green, characteristic of the emeraldine salt form of polyaniline. The solution was stirred for 20 h at room temperature. The precipitated $TiO_2$/PANI powder was filtered, washed with a solution of HCl (0.2 M) until yellowish washing waters turned uncolored, and dried at 80 ºC for 12 h.

*Platinum nanoparticles synthesis*

Platinum monometallic catalysts were supported on $TiO_2$/PANI and $TiO_2$/PPy. They were prepared by wet impregnation in excess of solvent, using $H_2PtCl_6 \cdot 6H_2O$ as the metal precursor. The proper amount of this salt to obtain 1 wt.% Pt loading was dissolved in ultrapure water, then the hybrid support ($TiO_2$/PANI/$K_2S_2O_8$, $TiO_2$/PPy/$K_2S_2O_8$ or

$TiO_2$/PPy/$FeCl_3$) was added (25 ml solution/g $_{support}$). The suspension was stirred for 12 h at room temperature and then the solvent was evaporated under reduced pressure in a rotary evaporator. The supported catalyst precursor was dried in an oven at 80 ºC for 12 h and then the obtained material was treated with Ar plasma to decompose the platinum precursor and obtain reduced platinum nanoparticles.

The plasma treatment proceeded as follows: the supported catalysts were loaded on an aluminum boat, which was placed in the glow discharge stainless steel cylindrical chamber of a Tucano plasma system (Gambetti Kenologia, Italy), provided with an anodized aluminum door. The HF electrode is made of aluminum and has a "Dark Shield", a RF 13.56 MHz power supply and mass flow controllers (MFC) for gas inlet control. The reaction chamber was evacuated to mild vacuum (0.2 mbar) using a Pfleiffer rotary vane pump (model PK D41 029C-Duo 2.5 with F4 Fomblin lubricant YL VAC 25/6). Ar (99.9999% minimum purity, Air Liquid) was introduced into the plasma chamber over the specimen (0.5 mbar). The plasma reactor was pumped down and purged for at least 10 min prior to activating the RF field. The discharge power was set to 200 watts and 36 cycles of 5 min each were applied to each sample (180 min treatment in total) with manual mixing of the sample between treatments to assure an even exposure to the plasma[27]. The temperature of the sample after the plasma treatment was measured by a non-contact infrared thermometer (PCE Instruments, model PCE-888). It could be determined that the surface temperature was below 50 ºC in all cases.

*Materials characterization*

Thermogravimetric analysis (TGA) was carried out in a SDT 2960 system (*TA Instruments*, Delaware, NC USA). TGA allowed determining the thermal stability of materials in nitrogen and in air. A heating ramp of 10 ºC/min and air or nitrogen flow of 100 mL/min were used. The weight of the samples was between 3-4 mg.

Textural characterization of polymers was carried out by $N_2$ adsorption at -196ºC with a coulter Omnisorp 100CX equipment. Samples were previously outgassed at 150ºC for 4 h.

Electrical conductivity was calculated from the resistance data. Electrical resistance of polypyrrole and polyaniline were determined in a home-made four-points probe equipment which consisted in a cylindrical Teflon sample holder, connected to a 2000 Multimeter (Madrid, Spain) through copper electrodes.

X-Ray diffraction (XRD) patterns of the polymers were obtained with a D8-Advance (Bruker) X-ray diffractometer equipped with Göebel mirror and a Cu anode, which provides Kα radiation (λ = 1.5406 Å). The samples were scanned from 2θ = 6 ° to 90 ° at the step scan mode (step size 1 °, step time 3 s).

Transmission electron microscopy (TEM) images were taken with a JEOL 2010 (JEOL Ltd., Tokyo Japan) equipment operating at 120 kV. Sample material was mounted on a holey carbon film supported on a Cu grid by drying a droplet of a suspension of ground sample in ethanol on the grid. EDX coupled to the TEM microscope provided elemental analysis of the samples.

X-ray photoelectron spectroscopy (XPS) analysis was used to obtain surface chemical information. A K-Alpha spectrometer (Thermo-Scientific) spectrometer with an Al $K_\alpha$ achromatic X-ray source (1486.6 eV) operating at 50 keV pass energy and 300 Watt was used. The pressure inside the analysis chamber was held below $5 \cdot 10^{-9}$ mbar during the course of the analysis. The measurements were taken using a take-off angle of 45º. Survey scans

were taken in the range 0-1350 eV, and high resolution scans were obtained on all significant peaks in the survey spectra. The intensities were estimated by calculating the integral of each peak, after subtraction of the S-shaped background, and by fitting the experimental curve to a combination of Lorentzian (30%) and Gaussian (70%) lines. Binding energies (B.E.) were referenced to the C 1s photopeak position for C-C and C-H species at 284.6 eV, which provided binding energy values with an accuracy of ± 0.2 eV.

*Nitrate removal evaluation*

The ability of removing nitrate from the aqueous solution by the titania/polymer hybrid materials was evaluated and compared with the hydrogenation of nitrate catalyzed by the platinum nanoparticles supported on these materials. A semi-batch reactor equipped with a magnetic stirrer (700 rpm) was fed with 592.5 mL of deionized water and 300 mg of hybrid material. $H_2$ was passed through the reactor only when the platinum catalyst was used. A $CO_2$ flow (75 mL·min$^{-1}$) was used as a buffer to keep a constant value of pH ≈ 5 during the reaction tests and minimize $NH_4^+$ production. 7.5 mL of a solution of $NaNO_3$ was added to the reactor (initial concentration of $NO_3^-$ in the reactor was 100 mg·L$^{-1}$). Aliquots (1 mL) were withdrawn at different times from the reactor and immediately filtered for determination of nitrate, nitrite and ammonium concentrations by ion chromatography using in a Metrohm 850 ProfIC AnCat-MCS equipment. Nitrate and nitrite anions were determined in a Metrosep ASSUPP-7 column (250 mm x 4 mm) and ammonium cation was determined in a Metrosep C3 column (250 mm x 4 mm).

Nitrate conversion ($X_{NO_3^-}$) and selectivities to nitrite ($S_{NO_2^-}$), ammonium ($S_{NH_4^+}$) and nitrogen ($S_{N_2}$) were determined using the following calculations:

$$X_{NO_3^-} = \frac{[NO_3^-]_0 - [NO_3^-]_t}{[NO_3^-]_0} \cdot 100$$

where $[NO_3^-]_0$ is the initial nitrate concentration (mg·L$^{-1}$) and $[NO_3^-]_t$ is the nitrate concentration (mg·L$^{-1}$) at time *t* (min).

$$S_{NO_2^-} = \frac{(n_{NO_2^-})_t}{(n_{NO_3^-})_0 - (n_{NO_3^-})_t} \cdot 100$$

$$S_{NH_4^+} = \frac{(n_{NH_4^+})_t}{(n_{NO_3^-})_0 - (n_{NO_3^-})_t} \cdot 100$$

The nitrogen gas phase was not analyzed, so $N_2$ selectivity was calculated from the balance of nitrite and ammonium analyzed in the solution, assuming that the production of $NO_x$ species is negligible[26].

$$S_{N_2} = 100 - S_{NO_2^-} - S_{NH_4^+}$$

When the reaction was performed in the presence of the platinum catalysts, a possible metal leaching was checked by Inducted Coupled Plasma Mass Spectrometry (ICP-MS) in aliquots withdrawn from the reactor once the nitrate reduction reaction was completed. A 7700x equipment (Agilent) was used: RF power 1150 W, He flow of 0.99 L/min and liquid flow of 0.3 mL/min).

## RESULTS AND DISCUSSION

### *Materials characterization*

The synthesized titania/polymer hybrid materials have been fully characterized and their properties compared to those of the pristine materials. Their thermal stability was evaluated by TGA in inert (Figure 1) and oxidizing (Supporting information Figure 1) atmospheres. Whereas $TiO_2$ does not suffer thermal degradation between 0-1200 ºC, both polymers show a first mass loss (around 8-9% of its initial mass) between 30 and 100 ºC which corresponds to the loss of water trapped in the polymers and the loss of non-reacted monomer. In PANI, thermal degradation in nitrogen atmosphere (Figure 1a) proceeds in several steps: there is a first step with a 10 % mass loss between 100-300 ºC which may correspond to the thermal dedoping of HCl and $K_2S_2O_8$.[50] Another 10 % mass loss is produced between 300-420 ºC where the polymer starts to decompose. The more pronounced thermal degradation between 420-600 ºC can be assigned to thermal degradation of the cross-linked chains; and the 40 % mass loss registered between 600- 1200 ºC is due to the decomposition of the lineal part of the chains. In PPy (Figures 1b and 1c), after the initial loss of water and unreacted polymer, there is a second mass loss between 100-250 ºC which is due to the loss of the dopant bound to the polymeric chains. At 250 ºC, degradation of the polymer starts, which proceeds in two steps, from 250 to 800 ºC which corresponds to the thermal degradation of the cross-linked chains and from 850 to 1200 ºC where degradation of the lineal part of the polymeric chains. The most important degradation in nitrogen atmosphere is produced for PPy synthesized with $K_2S_2O_8$ (10% mass remains) (Figure 1b); however, around 20% mass of PPy is retained when synthesized with $FeCl_3$ (Figure 1c). On the other hand, 28 % of PANI is not degraded (Figure 1a). In air atmosphere (Supporting

information Figure 1), total burning of PPy/$FeCl_3$ and PANI/$K_2S_2O_8$ is produced around 600 ºC, but it is produced at 730ºC for PPy/$K_2S_2O_8$.

These results show that the polymer nature and the oxidant used in the oxidative polymerization influence their final thermal properties. The thermal behavior of the hybrid materials is in between that of the polymer and that of $TiO_2$. The TGA curves show the mass loss steps corresponding to water and monomer loss, thermal dedoping and polymer degradation, but the increase of $TiO_2$ content decreases thermal degradation and increases the residual mass at 1200 ºC in nitrogen (Figure 1) and at 800 ºC in air (Supporting information Figure 1). Impregnation with platinum produces only a slight shift of the TGA curves of all the materials. Treatment with plasma does not significantly modify TGA curves (Supporting information Figure 2). From thermogravimetric analysis it can be concluded that application of the pristine polymeric materials may be restricted to temperatures below 250 ºC for PPy and 300ºC for PANI, but hybrid polymeric/$TiO_2$ materials have enhanced thermal properties.

The porous texture of the hybrid materials was evaluated by $N_2$ adsorption at 77 K. In all cases type II isotherms, typical of non-porous materials, were obtained (Supporting information Figure 3). Table 1 shows that BET surface areas of the hybrid materials prepared in a 50:50 $TiO_2$/polymer ratio are very similar (between 30-37 $m^2 \cdot g^{-1}$), irrespective of the polymer, and they are slightly lower than that of $TiO_2$ (53 $m^2 \cdot g^-1$) due to the polymer presence.

**Table 1.** BET surface evaluated from $N_2$ adsorption isotherms at 77 K.

| **Sample** | **$S_{BET}$ ($m^2 \cdot g^{-1}$)** |
|---|---|
| $TiO_2$ | 53 |
| PANI/$K_2S_2O_8$ | 40 |
| $TiO_2$/PANI/$K_2S_2O_8$/50:50 | 37 |
| PPy/$K_2S_2O_8$ | 11 |
| $TiO_2$/PPy/$K_2S_2O_8$/50:50 | 30 |
| PPy/$FeCl_3$ | 4 |
| $TiO_2$/PPy/$FeCl_3$/50:50 | 36 |

The XRD patterns of PANI and PPy (Figure 2) are typical of amorphous materials with a certain degree of crystallinity, which is shown by the band corresponding to the periodicity perpendicular to the polymer chain centered at 2θ = 30º for PANI; 2θ = 29.1º for PPy/$K_2S_2O_8$ and 2θ = 26.1º for PPy/$FeCl_3$.[51,52] In the XRD pattern of PANI there is also a band centered at 2θ = 18-20º that corresponds to the periodicity along the polymeric chain, and a third band situated at 2θ = 42º also typical of the polymer phase.[53] All the hybrid materials became strongly oriented, revealing a strong effect of the $TiO_2$, thus no amorphous bands from the polymer are shown. The XRD patterns of $TiO_2$/PANI and $TiO_2$/PPy show sharp and well defined peaks, indicating the crystallinity of all the synthesized hybrid materials, irrespective

of the monomer ratio. The more intense peak at 2θ = 25.3º corresponds to the (101) plane of anatase,[54] whereas the peaks at 37.8º, 48º, 54º and 63º correspond to (103), (200), (105) and (213) planes of this phase.[55] There is also a small reflexion from the (110) plane of rutile at 2θ = 28º.[56] In the platinum impregnated samples treated in plasma, reflexions from platinum (typically at 2θ = 39.8º and 46.2º ) are not present. [57] This may be due to a low percentage of metallic platinum or a high dispersion of the platinum nanoparticles[27].

TEM images (Figure 3) show that $TiO_2$ particles with diameters in the range between 10-50 nm are embedded in the polymer matrix, which leads to an oriented morphology. These results reveal that the improvement in crystallinity of hybrid materials is due to the addition of $TiO_2$ nanoparticles. During the synthesis of the nanocomposites, aniline or pyrrole monomers are adsorbed on the $TiO_2$ particles (Schemes 1a and 1b). With the addition of the oxidant polymerization starts, and growing polymer chains of different length surround and connect $TiO_2$ particles[58] as shown in Scheme 1c. Similar morphologies are obtained irrespective of the polymer (PANI or PPy) and the oxidant ($K_2S_2O_8$ or $FeCl_3$) (Supporting information Figures 4-6). As a result of the addition of the oxidant, the conducting protonated form of both polymers are obtained: protonated emeraldine salt in PANI (Scheme 1a) and conducting PPy (Scheme 1b). As nanoparticles usually tend to agglomerate due to the driving force to reduce their surface energy, it is crucial to assure the interaction of the conducting polymer with the $TiO_2$ nanoparticles at the nanometer scale as the uniform dispersion of $TiO_2$ nanoparticles into the polymeric matrix is a key factor. $TiO_2$ agglomeration is avoided by the repulsion between the positive charges of the conducting forms of the polymers.[59]

XPS analysis provides useful information about the surface composition of the different materials. XPS analysis of $TiO_2$ (Supporting information Table 1) shows the presence of Ti and O and also a considerable amount of C that may come from the precursor used in its preparation.[60–62] Carbon can also result from adventurous hydrocarbon. [63] XPS survey analysis of the composite materials shows the presence of C and N from the polymeric chain and Ti and O from titania. The increase of the polymer percentage in the hybrid materials results in an increase of N and C and a decrease of Ti and O in the three studied series ($TiO_2$/PANI/$K_2S_2O_8$, $TiO_2$/PPy/$K_2S_2O_8$ and $TiO_2$/PPy/$FeCl_3$) (Supporting information Table 1).

High resolution XPS spectra show variations of Ti, O, C, and N binding energies of the hybrid materials when compared to the pristine titania and polymers. Ti $2p_{3/2}$ curve fit (Figure 4, Supporting information Table 2) shows the unique contribution of $Ti^{4+}$ at 458.9 eV in pristine $TiO_2$. In the hybrid materials, the Ti $2p_{3/2}$ binding energy is shifted towards higher values (459.5 eV). No contribution of $Ti^{3+}$ (456-457 eV) is shown in any hybrid material, which is in agreement with the literature.[64]

The electron transfer between titania and the polymer depends on both the oxidation state of titanium and the degree of oxidation of the polymeric chain. This can be determined by the binding energy of the N 1s level. Four types of nitrogen may be present: imine (-N=), neutral amine (-NH-), positively charged nitrogen ($-N^+$) and protonated imine ($=N^+$), with increasing N 1s binding energies, typically located at 398.9, 399.6, 400.9 and 401.8 eV, as the oxidation degree increases. XPS high resolution curve fit of the N 1s level (Figure 5,

Supporting information Table 3) shows by the presence of positively charged amine ($-N^+$), this confirming that the conducting form of the polymers have been obtained.

The formation of the $TiO_2$/PANI hybrid material does not greatly affects the oxidation degree of the polymeric nitrogen ($N^+$ moieties percentage is 17% in the pristine PANI/$K_2S_2O_8$ and 15% in the hybrid material $TiO_2$/PANI/$K_2S_2O_8$). On the other hand, pristine polypyrrole is more oxidized than pristine polyaniline. However, the percentage of positively charged nitrogen ($-N^+$) in PPy depends on the oxidant used during the chemical polymerization of pyrrole (93% with $K_2S_2O_8$ versus 65% with $FeCl_3$) (Supporting information Table 3). These results reveal that the oxidant used in the polypyrrole synthesis has a considerable influence on the oxidation degree of the polymeric material and consequently, on its final properties. Whereas N1s curve fit is similar in PANI and in the $TiO_2$/PANI hybrid material (Figure 5a), a significant modification of the nitrogen functionalities is observed in the $TiO_2$/PPy hybrid materials. The imine (=N-) groups of the pristine polymer are no longer present in $TiO_2$/PPy/$K_2S_2O_8$, (Figure 5b) and protonated imine ($=N^+$) moieties are detected in $TiO_2$/PPy/$FeCl_3$ (Figure 5c). The shift of the binding energies of N 1s of PPy to lower binding energies are produced together with a shift of Ti $2p_{3/2}$ to higher binding energies. C 1s and O 1s binding energies are also shifted towards lower binding energies by the presence of $TiO_2$.

C1s curve fits of the hybrid materials with a 50:50 titania/polymer ratio (Figure 6, Supporting information Table 4) show the presence of C-C, C-H and C-N species from the polymer. Some C-O and C=O moieties are created as a result of the reaction of the polymer surface with water and air[27]. Some of these oxygenated moieties may also correspond to

benzoquinone and hydroquinone species in PANI as a result of an excessive oxidation of polyaniline.[65] These O-C and O=C species are also observed in the O 1s high resolution XPS spectra (Figure 7, Supporting information Table 5). O 1s curve fit also shows the presence of hydroxyl groups due to the exposure of $Ti^{4+}$ sites to water in air.[14]

C 1s contributions of PANI/$K_2S_2O_8$ at 284.7 and 286.7 eV (Figure 6, Supporting information Table 4) are shifted towards lower binding energies (284.6 and 285.9 eV) when PANI is a part of the hybrid material ($TiO_2$/PANI/$K_2S_2O_8$/50:50). In $TiO_2$/PPy this shift towards less oxidized polymeric carbon is more evident in the presence of $FeCl_3$. Thus, C 1s contributions at 284.9 and 286.3 eV in PPy/$FeCl_3$ are shifted to 284.2 eV and 285.3 in the $TiO_2$/PPy/$FeCl_3$/50:50 hybrid. There is also a shift of the O 1s contributions in the pristine polymers towards lower binding energies in the hybrid materials (Figure 7, Supporting information Table 5). The shifts of the binding energies of C 1s and O 1s of the polymers to lower binding energies are produced together with a 0.6-0.8 eV shift of Ti 2p to higher binding energies in all hybrid materials. This evidences the existence of Ti-C and Ti-O-C interactions in the hybrid material. O 1s curve fit of $TiO_2$ (Figure 7, Supporting information Table 5) shows a peak at 530.0 eV, which is ascribed to O-Ti bond in the oxide, and another peak at 532.0 eV which corresponds to the surface hydroxyl (O-H) of water adsorbed on $TiO_2$. Therefore, hydrogen bond between surface hydroxyl groups in titanium dioxide and nitrogen in the polymer might also take place. The Ti-O-C and Ti-C interactions at the interface between the titanium particles and the polymers may favor the electron transfer in the hybrid materials.[30,64,66]

$TiO_2$ is a non-conducting solid. Otherwise, the hybrid $TiO_2$/polymer materials showed higher conductivities due to their polymeric counterpart. The oxidation degree of the polymer determines the electrical properties of the hybrid material. Table 2 shows considerably high conductivity values of the materials containing PANI and also PPY synthesized with $FeCl_3$. However, the conductivities of the hybrid materials containing PPy synthesized with $K_2S_2O_8$ are considerably lower, which is indicative of a lower degree of oxidation of the pyrrolic N (Scheme 1b).

**Table 2.** Conductivity measured on the materials.

| ***Material*** | ***Conductivity*** $(S \cdot m^{-1})$ |
|---|---|
| $TiO_2$ | $3.5 \cdot 10^{-5}$ |
| $PANI/K_2S_2O_8$ | 47.5 |
| $TiO_2/PANI/K_2S_2O_8$ | 46.2 |
| $H_2PtCl_6/TiO_2/PANI/K_2S_2O_8$ | 32.5 |
| $Pt/TiO_2/PANI/K_2S_2O_8$ | 0.26 |
| $PPy/K_2S_2O_8$ | $1.2 \cdot 10^{-1}$ |
| $TiO_2/PPy/K_2S_2O_8$ | $5.4 \cdot 10^{-2}$ |
| $H_2PtCl_6/TiO_2/PPy/K_2S_2O_8$ | $4.5 \cdot 10^{-3}$ |
| $Pt/PPy/K_2S_2O_8$ | $6.6 \cdot 10^{-4}$ |
| $PPy/FeCl_3$ | 130.9 |
| $TiO_2/PPy/FeCl_3$ | 64.4 |

| | |
|---|---|
| $H_2PtCl_6/TiO_2/PPy/FeCl_3$ | 50.0 |
| $Pt/TiO_2/PPy/FeCl_3$ | 1.5 |

However, the percentage of positively charged nitrogen in the polymeric matrix determines not only the redox properties but also the ion exchange ability of the hybrid material. $FeCl_3$ and $K_2S_2O_8$ oxidants not only produce a different degree of oxidation of the polymeric chain, which determines its capability for donating electrons, but they also provide the semioxidized polymeric chain with different counter-ions which neutralize the positive charge of the $N^+$ moieties. $K_2S_2O_8$ is responsible for the introduction of O and S moieties detected on both, $TiO_2/PPy/K_2S_2O_8$ and $TiO_2/PANI/K_2S_2O_8$ (Supporting information Table 1). The binding energy of the S 2p peak (168.3 eV) corresponds to sulfate ion, which is produced as a result of the reduction of persulfate ($S_2O_8^{2-}$) to sulfate ($SO_4^{2-}$), upon its incorporation as a counter-ion during the oxidative polymerization of aniline and pyrrole with potassium peroxydisulfate. When ferric chloride is used, chlorine ion is detected in $PPy/FeCl_3$ (Cl 2p at 198.5 eV); but it is also detected on PANI synthesized with $K_2S_2O_8$ in HCl medium. This suggests that Cl from HCl is also introduced as a counterion in PANI. A certain amount of Cl has also been detected on PPy synthesized with $K_2S_2O_8$. In this case, Cl may be ascribed to chloride from the aqueous medium. Neither K from $K_2S_2O_8$ nor Fe from $FeCl_3$ are detected, which confirms that cations do not anchor to the oxidized polymeric chains during the oxidative polymerization of aniline and pyrrole. Chloride and sulfate counteranions are anchored to the semioxidized polymeric chain and therefore they can be potentially exchanged by nitrate present in the aqueous solution (Scheme 2). The higher

percentage of oxidized amine $N^+$ moieties, the higher amount of counterions ($A^-$ in Schemes 1 and 2) susceptible of being exchanged by nitrate. From this point of view $TiO_2$/PPy/$K_2S_2O_8$, which shows a relatively low conductivity (Table 2) and only contains sulfate as counterion to neutralize a relatively low percentage of $N^+$ moieties, is expected to have a limited performance in the adsorption of nitrate from the aqueous solution compared to $TiO_2$/PPy/$FeCl_3$ and $TiO_2$/PANI/$K_2S_2O_8$.

As stated before, the goal of this study is to prepare metal-free materials able of adsorbing aqueous nitrate and produce its selective reduction to nitrogen. For comparison purposes, the synthesized materials were also used as support of platinum nanoparticles and tested in the catalytic hydrogenation of nitrate. The performance of the metal and the metal-free materials in the removal of nitrate from the aqueous solution was compared.

To prepare the supported platinum catalysts, the hybrid titania/polymer materials were impregnated with hexachloroplatinic acid ($H_2PtCl_6$) in a first step. As a result, a chloroplatinum complex anchors to the N functionalities of the polymeric chain, as it has been previously reported.[67] During the formation of the coordination compound, $Pt^{4+}$ from $H_2PtCl_6$ is partially reduced to $Pt^{2+}$. The reduction of platinum ion is produced by the electrons coming from the polymeric chain through the N functionality (Scheme 3a-b).This is more evident in the composite with PANI, where only $Pt^{2+}$ is detected after the impregnation of the material with $H_2PtCl_6$ (Figure 8a), and this is accompanied by an increase in the amount of $N^+$ functionalities (Figure 5a). This is explained by the fact that, before being treated with the platinum precursor, $TiO_2$/PANI/$K_2S_2O_8$ is less oxidized (there is a less

important percentage of oxidized amine functionalities) than the composites with PPy (Figures 5b and 5c). As a result, 100 % of platinum ion is reduced to $Pt^{2+}$ and no contribution of $Pt^{4+}$ is shown in $H_2PtCl_6/TiO_2/PANI/K_2S_2O_8$. However, platinum ions in different oxidation states are present in the composites with PPy after impregnation with $H_2PtCl_6$ (Figure 8a).

The hydrogenation of nitrate requires a noble metal as catalyst. In order to produce metal platinum nanoparticles, the materials impregnated with $H_2PtCl_6$ were treated in cold Ar plasma in a second step. Formation of platinum nanoparticles implies dissociation of the platinum complexes anchored to the polymeric chain through the nitrogen functionality ($-N^+---[PtL_4]^{2-}$) (Scheme 3). As a result, the oxidation state of the polymeric chain is affected as assessed by N 1s contributions: (Figure 5 and Supporting information Table 3). The ligands released from the dissociated platinum complex ($L^{n-}$) could act as counteranions to stabilize the oxidized polymeric chain. In the case of PANI support, platinum ions (as $Pt^{2+}$) anchored to $N^+$ moieties located out of the aromatic ring in PANI are more easily reduced to metallic $Pt^0$ by the high energy electrons in the plasma than platinum ions anchored to $N^+$ located inside the ring in PPy. Therefore, considerably higher amount of metallic platinum is detected on PANI surface (80%) compared to PPy (44-59%) after plasma treatment (Supporting information Table 6). This significant lower metallic Pt loading than the theoretical value of 1 wt.% together with a high dispersion of the Pt nanoparticles is in agreement with the absence of Pt peaks in XRD patterns (Figure 2) TEM micrographs showed that the platinum nanoparticles (detected by EDX) of 2-5 nm diameter are mainly located on the polymer chains that connect $TiO_2$ particles (Figure 3d, Supporting information

Figures 4d, 5d and 6 d). In all cases, the deposition of platinum nanoparticles lowered the conductivity of the materials (Table 2).

***Nitrate removal from water***

The mechanism of removing nitrate from water by the synthesized metal-free hybrid materials has been assessed and compared to the hydrogenation of nitrate catalyzed by Pt nanoparticles supported on the titania/polymer hybrid materials.

i) *Reduction of nitrate by metal-free hybrid materials*

Aliquots were withdrawn from the nitrate solution in contact with the hybrid $TiO_2$/polymer hybrid materials at different times (1, 5, 10, 15, 20, 25, 30, 45, 60, 90, 120, 180, 240, 300 min). The nitrate abatement was rapidly achieved and after 5 min the measured concentrations of nitrate and ammonium remained constant (Supporting information Figure 7). Nitrite concentrations below 0.1 $mg \cdot L^{-1}$ were detected in all cases. Figure 9 shows concentrations measured after 5 minutes of reaction. The metal-free hybrid materials ($TiO_2$/PPy/$FeCl_3$ and $TiO_2$/PANI/$K_2S_2O_8$) produce an effective abatement of nitrate from water (almost 70%) in just 5 minutes (Figure 9a), resulting in measured nitrate concentrations around 30 $mg \cdot L^{-1}$, (Supporting information Table 7) which accomplishes with the legislation (less than 50 $mg \cdot L^{-1}$)[1,2]. However, only 40% of nitrate is abated in the presence of $TiO_2$/PPy/$K_2S_2O_8$. This evidences a determinant role of the counterion provided by the oxidant. As PPy synthesis is carried out by the oxidative polymerization of the pyrrole monomer on the $TiO_2$ in a neutral aqueous medium; either chloride or sulfate anions from the oxidants ($FeCl_3$ or $K_2S_2O_8$) are introduced (Scheme 1b). Otherwise, during the PANI

synthesis in HCl medium, the anilinium cation is formed in a first step and is then oxidized by the potassium peroxidisulfate (Scheme 1a). As a result, both chloride and sulfate counteranions are introduced to neutralize the positively charged polyaniline chain.

The relative size of the dopant anions has a key role in the exchange with nitrate from the solution. Considering the relative size of the chloride anion (ionic radius 181 pm) and the thermochemical radii of $NO_3^-$ (179 pm) and $SO_4^{2-}$ (258 pm),[68] it is expected the exchange of chloride ion by aqueous nitrate to be easier than the exchange of sulfate ion. Once nitrate has been adsorbed on the polymeric matrix of the material, it must be reduced to assure proper removal without the concern of a further disposal of adsorbed nitrate. XPS revealed the transfer of electrons from titania to the polymer, so the polymer counterpart in the hybrid material is responsible for the reduction of nitrate. Actually, the reduction potentials of nitrate ($NO_3^-/NH_4^+$, $E^o$ = +0.875 V; $NO_3^-/N_2$, $E^o$ = +1.246 V), polyaniline (emeraldine/leucoemeraldine, $E^o$ = +0.342 V; pernigraniline/emeraldine, $E^o$ = + 0.942 V) and polypyrrole ($PPy^+/PPy$, $E^o$ = +0.150 V) are consistent with the reduction of adsorbed nitrate produced by the electrons coming from the polymeric matrix.

However, the mechanism is still unclear. If electrons keep flowing from $TiO_2$ to nitrate through the conducting polymer, some species must be supplying them, otherwise the continuity will not be there. Challagulla et al.[72] compared the photocatalytic nitrate reduction mechanism over $Pt/TiO_2$ with the non-photocatalytic nitrate reduction experiments in dark using doped and undoped $TiO_2$ catalysts both with and without purging of $H_2$ gas. They stated

that the valence band of $TiO_2$ lies in the suitable range to oxidize species such as hydroxide to hydroxyl radical whereas the conducting band lies in the suitable range to reduce various species like nitrate, nitrite, etc. From our experience, the catalytic reduction of nitrate is being produced by the electrons flowing from $TiO_2$ through the polymer. Although the precise origin of the continuous electron supply is unclear, it might be plausible that electrons could arise from the photocatalytic oxidation of water, with titania or the whole hybrid acting as a photocatalyst. Nevertheless, further research work is being carried out to unearth the reduction mechanism.

Figure 9a shows that the most effective removal of nitrate (around 70%) is produced by $TiO_2$/PANI/$K_2S_2O_8$ and $TiO_2$/PPy/$FeCl_3$. Both materials have chloride counter-ions and are more oxidized than $TiO_2$/PPy/$K_2S_2O_8$, as determined by XPS and conductivity measurements. Consequently, nitrate exchange and nitrate reduction produced by those materials are favored in comparison with $TiO_2$/PPy/$K_2S_2O_8$. In all cases nitrite ($NO_2^-$) concentrations are below 0.15 $mg \cdot L^{-1}$ and satisfy the quality standards for potable water (legislation stablishes maximum permitted concentrations of nitrate, nitrite and ammonium less than 50, 0.5 and 0.5 $mg \cdot L^{-1}$, respectively). These low measured nitrite concentrations confirm that nitrite does not get into the solution followed by re-adsorption by the support. On the contrary, intermediate nitrite is rapidly reduced to ammonium, in the presence of $TiO_2$/PPy/$K_2S_2O_8$; or to nitrogen, in the presence of $TiO_2$/PANI/$K_2S_2O_8$ and $TiO_2$/PPy/$FeCl_3$, where ammonium concentrations below 0.2 $mg \cdot L^{-1}$ are detected.

Recyclability of the hybrid materials was tested. Thus, after 300 min of reaction, when the first run was completed, the materials were separated by centrifugation and put into contact with a 1M solution of NaCl during 30 min under stirring. The purpose of that was to exchange possibly adsorbed nitrate ions with chloride ions and regenerate the polymer counterpart in the hybrid material. Then, the materials were introduced in the reactor containing a fresh nitrate solution for subsequent runs under identical conditions. The measured concentrations of nitrate, nitrite and ammonium measured after 300 min of each run are summarized in Supporting information Table 7. Nitrate conversions achieved with the regenerated materials were only slightly lower than those obtained during the first run. Similar ammonium selectivities were obtained and nitrite was not detected in any case. XRD and TEM of the recovered materials (not shown) remained almost unchanged, so no morphological changes were produced.

*ii) Hydrogenation of nitrate catalyzed by Pt supported on the hybrid materials*

Catalytic reduction of nitrate ($NO_3^-$) with dyhidrogen ($H_2$) progresses through intermediate nitrite ($NO_2^-$) towards either nitrogen ($N_2$) or ammonium ($NH_4^+$) as final products:

$$NO_3^- + H_2 \rightarrow NO_2^- + H_2O \quad (1)$$

$$NO_2^- + 3/2\ H_2 \rightarrow ½\ N_2 + H_2O + OH^- \quad (2)$$

$$NO_3^- + 4H_2 \rightarrow NH_4^+ + H_2O + 2OH^- \quad (3)$$

$$NO_2^- + 3H_2 \rightarrow NH_4^+ + 2OH^- \quad (4)$$

As a consequence of hydroxyl formation, there is an increase of the pH of the solution up to 10-11, which is unacceptable for drinking water, and favors the selectivity towards ammonium instead of nitrogen.[69,70] This is minimized by buffering the solution with a $CO_2$ flow. Considering toxicity of nitrite and ammonium, selective reduction of nitrate towards nitrogen is necessary to accomplish legislation.

Figure 9a shows no activity of the platinum catalyst supported on titania. However, between 30-40 % of the total nitrate is abated in the presence of the platinum catalysts supported on the hybrid materials, which measured nitrate concentrations over 60 $mg \cdot L^{-1}$ (Supporting information Table 7). ICP-MS results (Supporting information Table 8) show that platinum leaching was not produced as lixiviated platinum was always less than 0.1%.

Due to the presence of the conducting polymeric matrix in the composite, the mechanism of reduction of aqueous nitrate catalyzed by platinum nanoparticles supported on the $TiO_2$/polymer hybrid materials may differ from the reported mechanisms for nitrate reduction with $H_2$ catalyzed by Pt or Pd supported on $TiO_{2.<sup>14</sup>}$ Yoshinaga et al.[71] reported that as palladium is very active for hydrogenation reactions, the nitrate and the nitrite molecules produced by the reduction of nitrate, would be deeply hydrogenated producing ammonium, as shown in reactions (3) and (4). However, Figure 9 shows higher activity and lower ammonium selectivity when the metal-free hybrid materials are used. Therefore, platinum deposition on all the studied materials decreases nitrate removal efficiency. It is reported[14] that in $Pd/TiO_2$ systems nitrate is adsorbed at the Lewis acid sites on titania

following exchange with $OH^-$ anions. Nitrate is then reduced by $Ti_4O_7$ species and nitrite is preferentially reduced by Pd. Challagulla et al.[72] reported the competitive nature between nitrate reduction and hydrogen generation in the presence of platinum doped $TiO_2$. In our experience, no nitrate abatement is significantly produced in the presence of $Pt/TiO_2$. However 30-40 % of nitrate is removed by the platinum catalysts supported on $TiO_2$/conducting polymer hybrid materials. In these materials, the electron transfer from the conducting polymer to nitrate ions through the nitrogen functionalities is limited due to the anchoring of the platinum chlorocomplexes (Scheme 3d). This results in a considerable decrease of the amount of the adsorbed nitrate. In this case, nitrate reduction is mainly produced by dihydrogen and catalyzed by the metal platinum nanoparticles dispersed on the hybrid materials. Otherwise, in the metal-free hybrid materials, the electrons are directly transferred from the polymeric matrix to adsorbed nitrate, producing its reduction (Scheme 2). The presence of $TiO_2$ in the composite material not only enhances its thermal properties but also modifies the oxidation state of the polymeric matrix, due to the transfer of electrons from titania to the semi-oxidized polymeric chain. Thus, the reductive ability of the polymeric matrix, that is, its capability of transferring electrons to the adsorbed nitrate ions is increased.

## CONCLUSIONS

A new route for abating nitrate from water and produce its selective reduction towards nitrogen, avoiding the use of a metal catalyst and gaseous hydrogen, has been developed. This implies the use of titanium dioxide/conducting polymer hybrid materials. During their synthesis, aniline and pyrrol polymerize on titanium dioxide surface connecting titanium

dioxide particles. As a result, conducting hybrid materials with enhanced thermal properties are obtained. These materials are capable of adsorbing nitrate and subsequently produce its reduction. The oxidant used during the polymerization of the monomers onto titania plays a key factor as the degree of oxidation of the polymeric chain imparted by the oxidant affects the amount of counterions susceptible to be exchanged by nitrogen. The size of the counterion also determines the effective exchange with nitrate. Ti-C and Ti-O-C interactions between the polymers and titanium dioxide allows the electron transfer from titania to the polymer chain, which produce the reduction of the adsorbed nitrate.

Nitrate reduction produced by $TiO_2$/PPy/$FeCl_3$ and $TiO_2$/PANI/$K_2S_2O_8$ is considerably more effective than the catalytic hydrogenation produced by platinum nanoparticles supported on these composite materials. In the metal-free composites, the reduction of nitrate is produced by the electrons provided directly by the hybrid material. Otherwise, there is a considerable decrease in the activity of the nitrate reduction reaction produced by the materials containing platinum. The loading of the hybrid materials with platinum results in the blocking of N sites by Pt. Therefore, the transfer of electrons from the material to nitrate adsorbed to the polymeric chain by ion exchange is diminished, and the reduction of nitrate is mainly produced by the dihydrogen dissolved in water and adsorbed on Pt nanoparticles. Nevertheless, both mechanisms might be having a role in the platinum loaded materials: not only a catalytic hydrogenation is taking place but it could also be a contribution of the electrons provided by the polymer to the reduction of nitrate.

# FIGURES

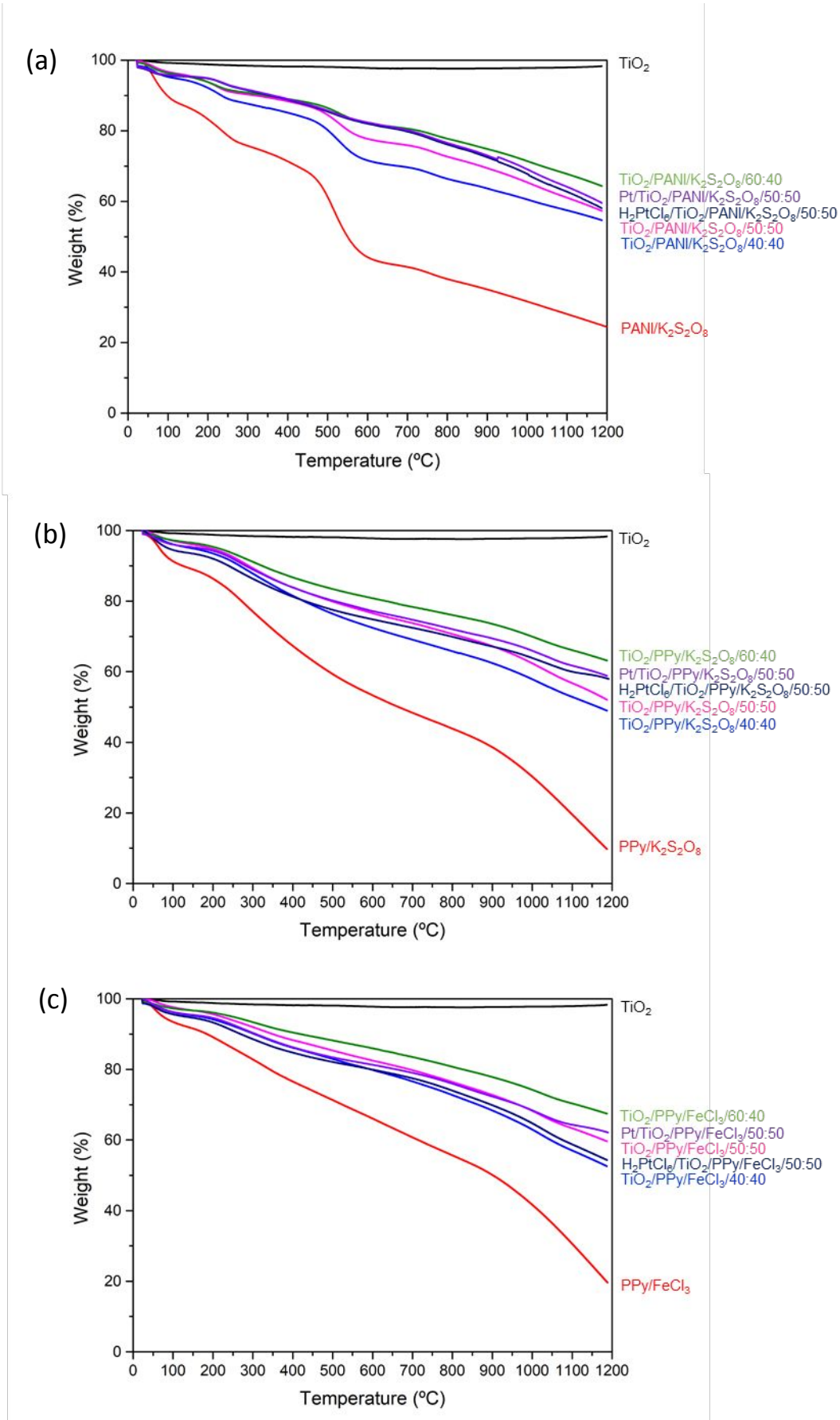




**Figure 1.** TGA profiles in nitrogen atmosphere of (a) $TiO_2$/PANI/$K_2S_2O_8$; (b) $TiO_2$/PPy/$K_2S_2O_8$; (c) $TiO_2$/PPy/$FeCl_3$.

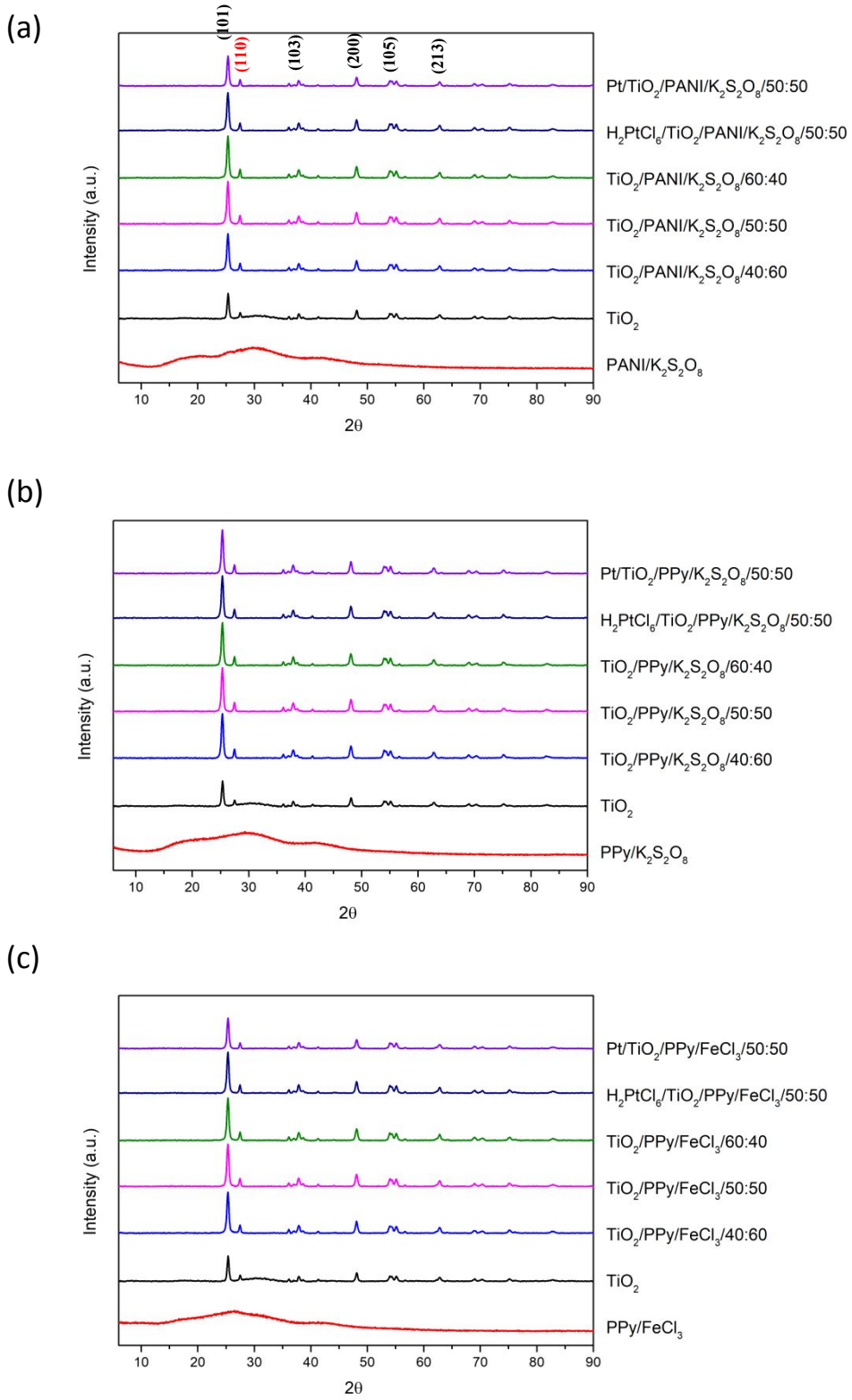


**Figure 2.** XRD diffraction patterns of hybrid materials (a) $TiO_2/PANI/K_2S_2O_8$; (b) $TiO_2/PPy/K_2S_2O_8$; (c) $TiO_2/PPy/FeCl_3$.

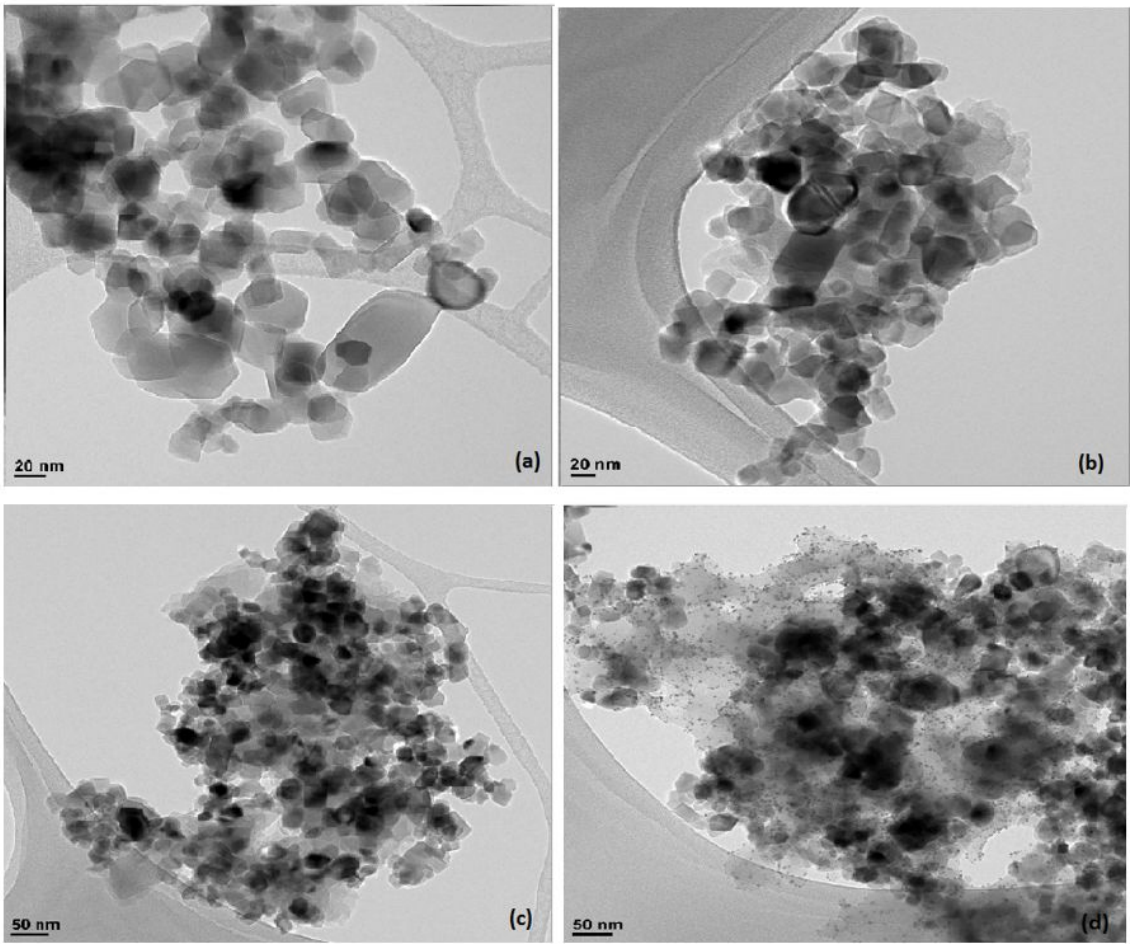


**Figure 3.** TEM images (a) $TiO_2$; (b) $TiO_2$/PANI/50:50; (c) $H_2PtCl_6$/$TiO_2$/PANI; (d) Pt/$TiO_2$/PANI.

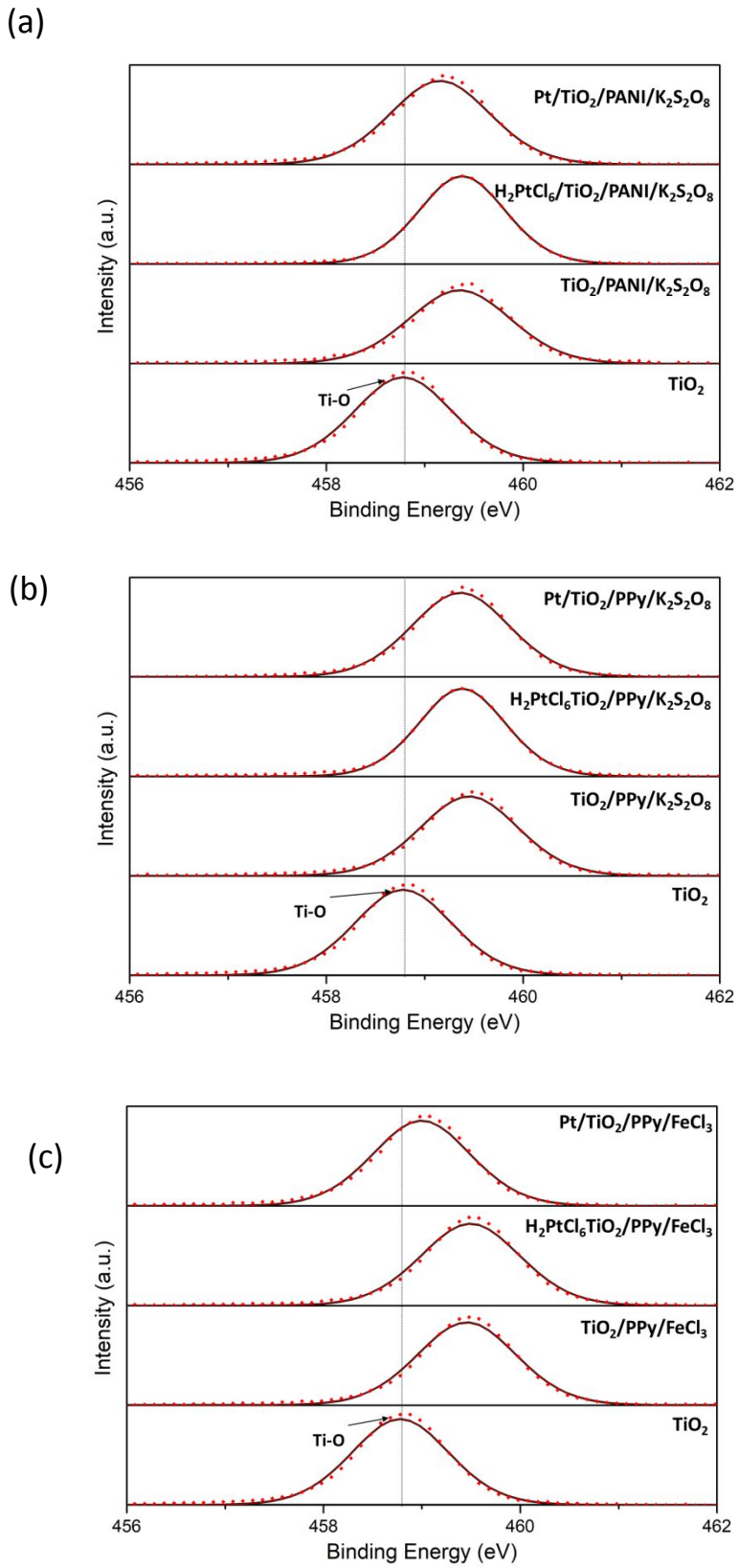


**Figure 4.** XPS Ti 3d spectra of (a) $TiO_2$/PANI with $K_2S_2O_8$ and $TiO_2$/PPy with (b) $K_2S_2O_8$ or (c) $FeCl_3$.

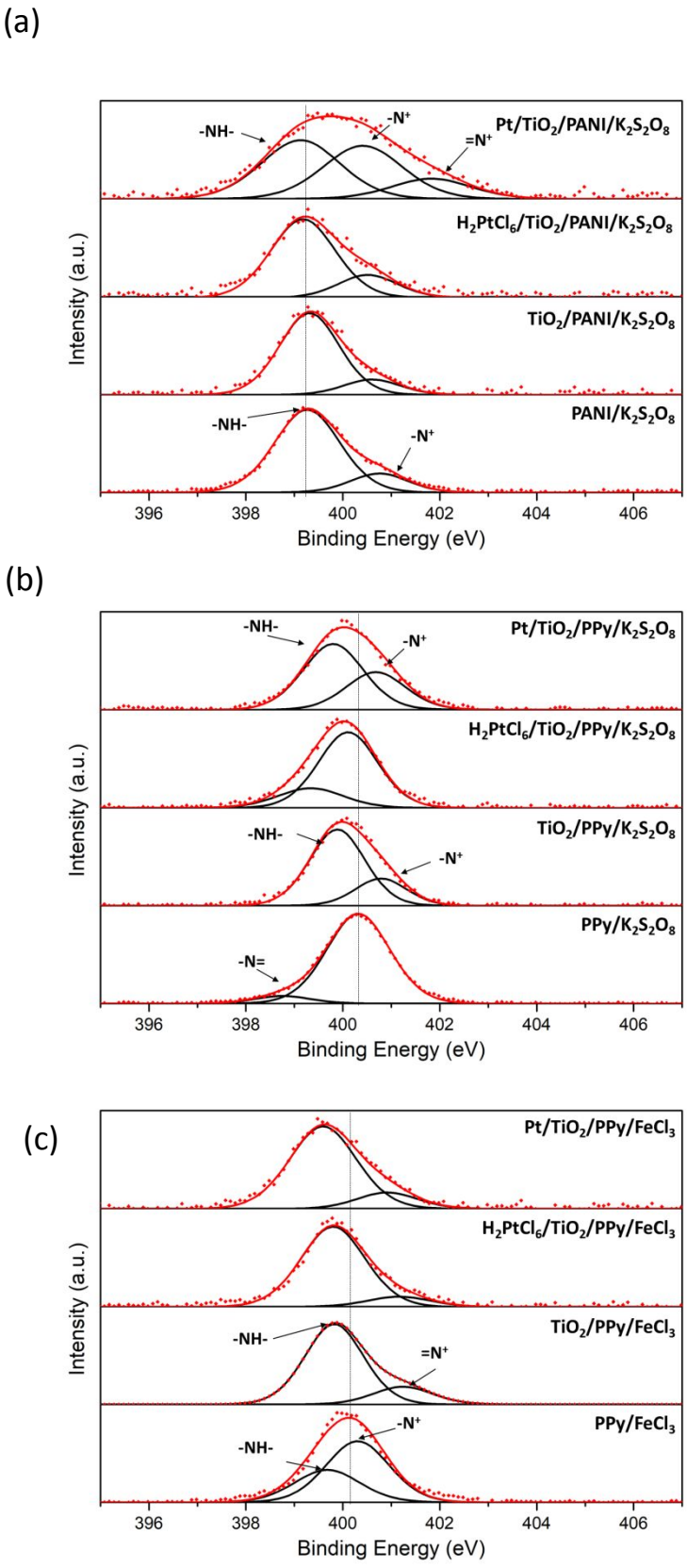


**Figure 5.** XPS N 1s spectra of (a) $TiO_2$/PANI with $K_2S_2O_8$ and $TiO_2$/PPy with (b) $K_2S_2O_8$ or (c) $FeCl_3$.

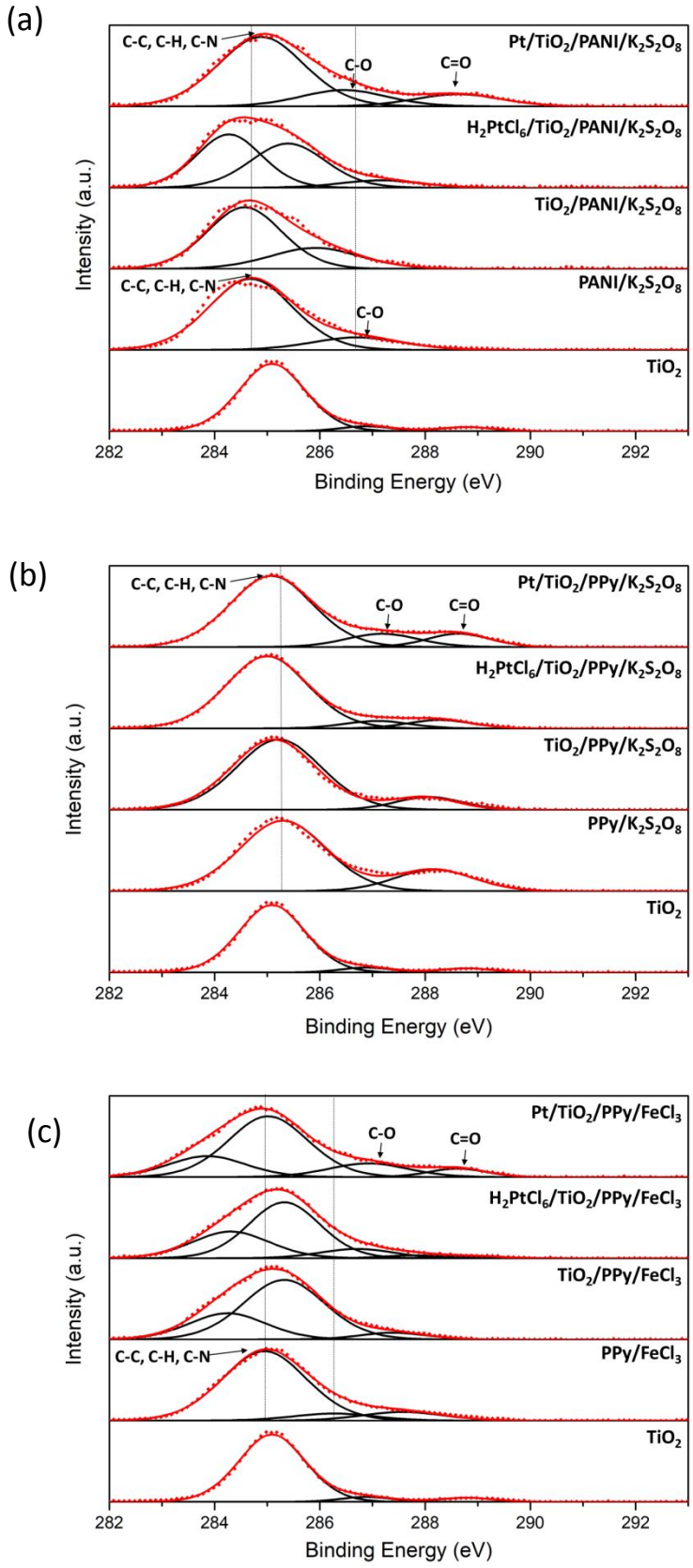


**Figure 6.** XPS C 1s spectra of (a) $TiO_2$/PANI with $K_2S_2O_8$ and $TiO_2$/PPy with (b) $K_2S_2O_8$ or (c) $FeCl_3$.

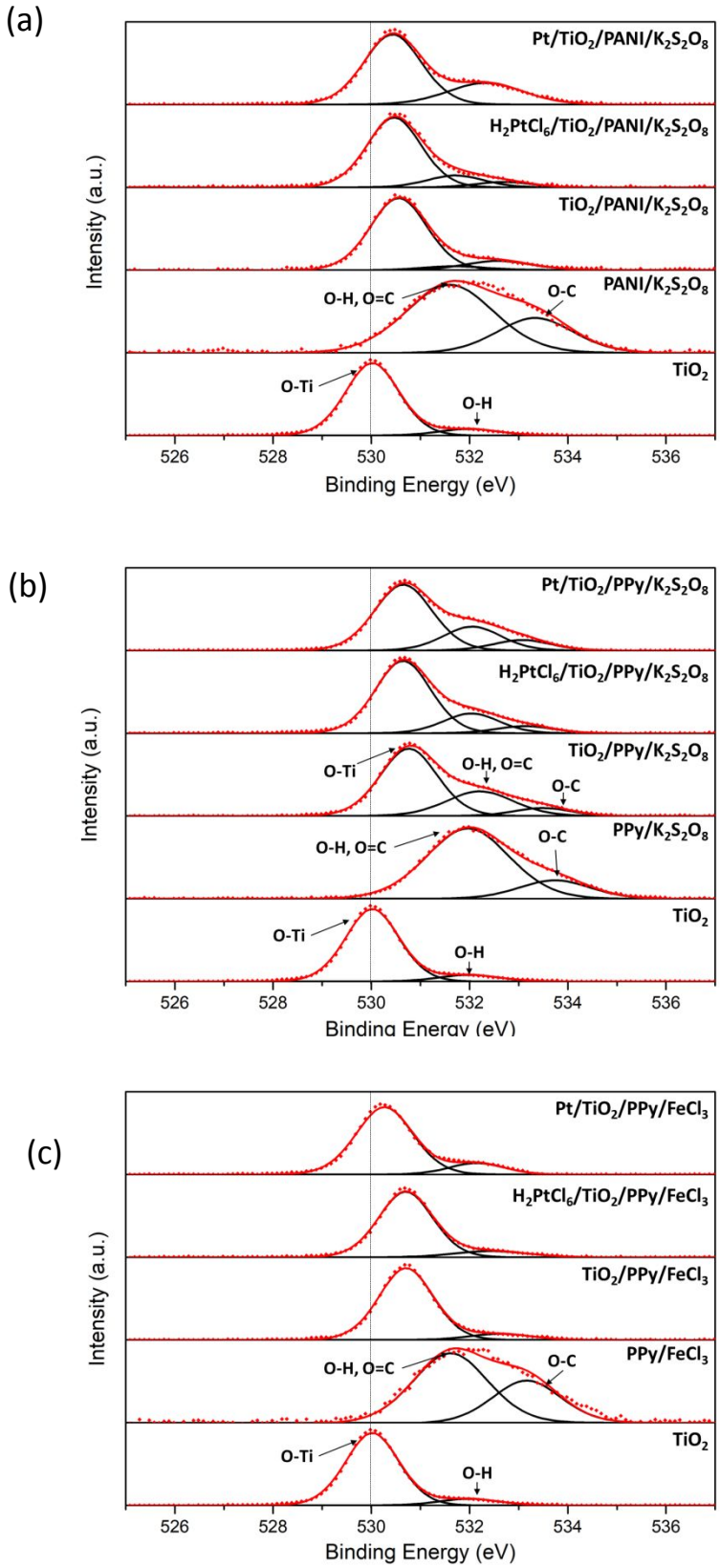


**Figure 7.** XPS O 1s spectra of (a) $TiO_2$/PANI with $K_2S_2O_8$ and $TiO_2$/PPy with (b) $K_2S_2O_8$ or (c) $FeCl_3$.

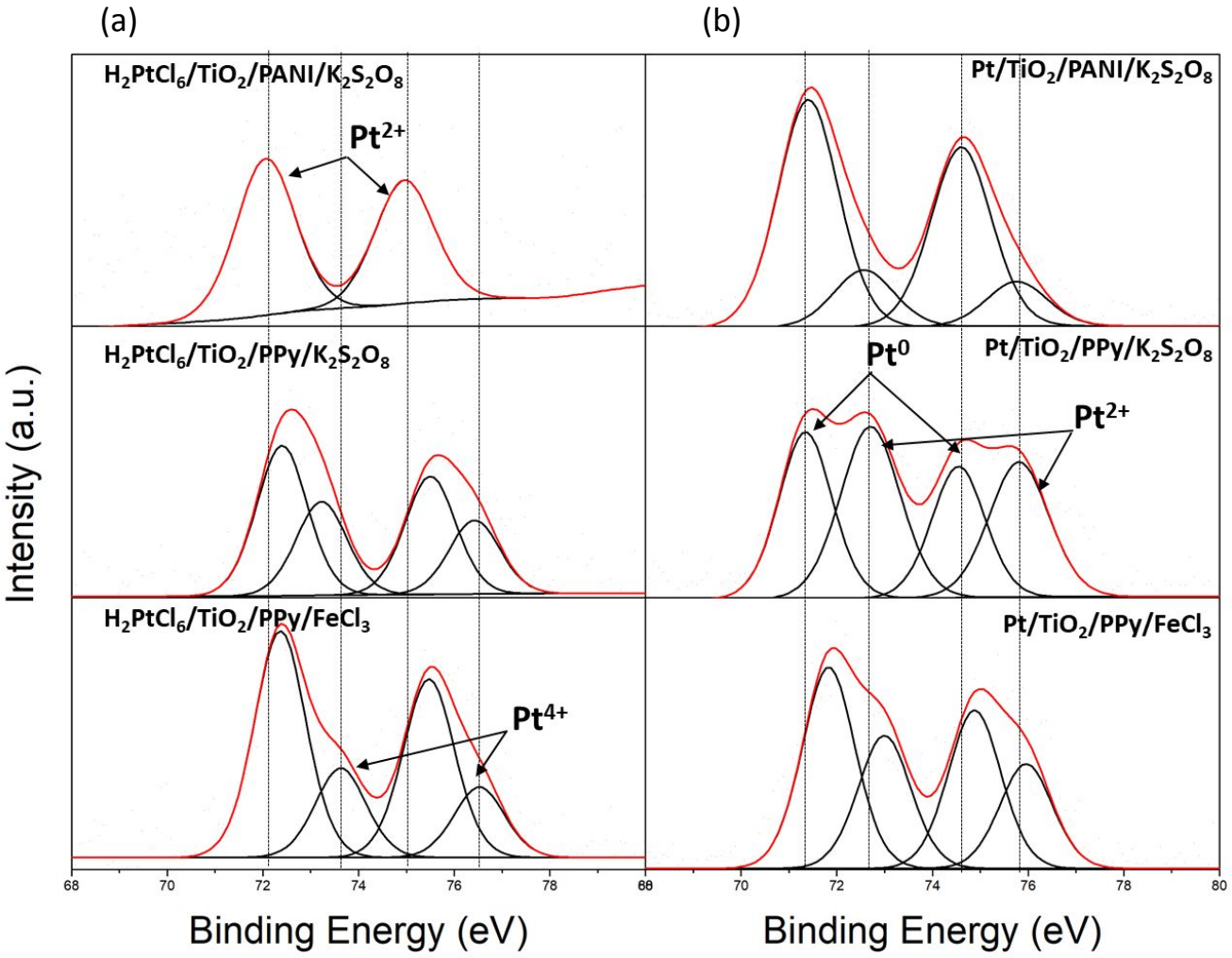


**Figure 8.** XPS Pt 4f spectra of $TiO_2$/PANI/$K_2S_2O_8$ and $TiO_2$/PPy/$FeCl_3$ or $K_2S_2O_8$ (a) after impregnation with $H_2PtCl_6$; (b) after a reductive plasma treatment.

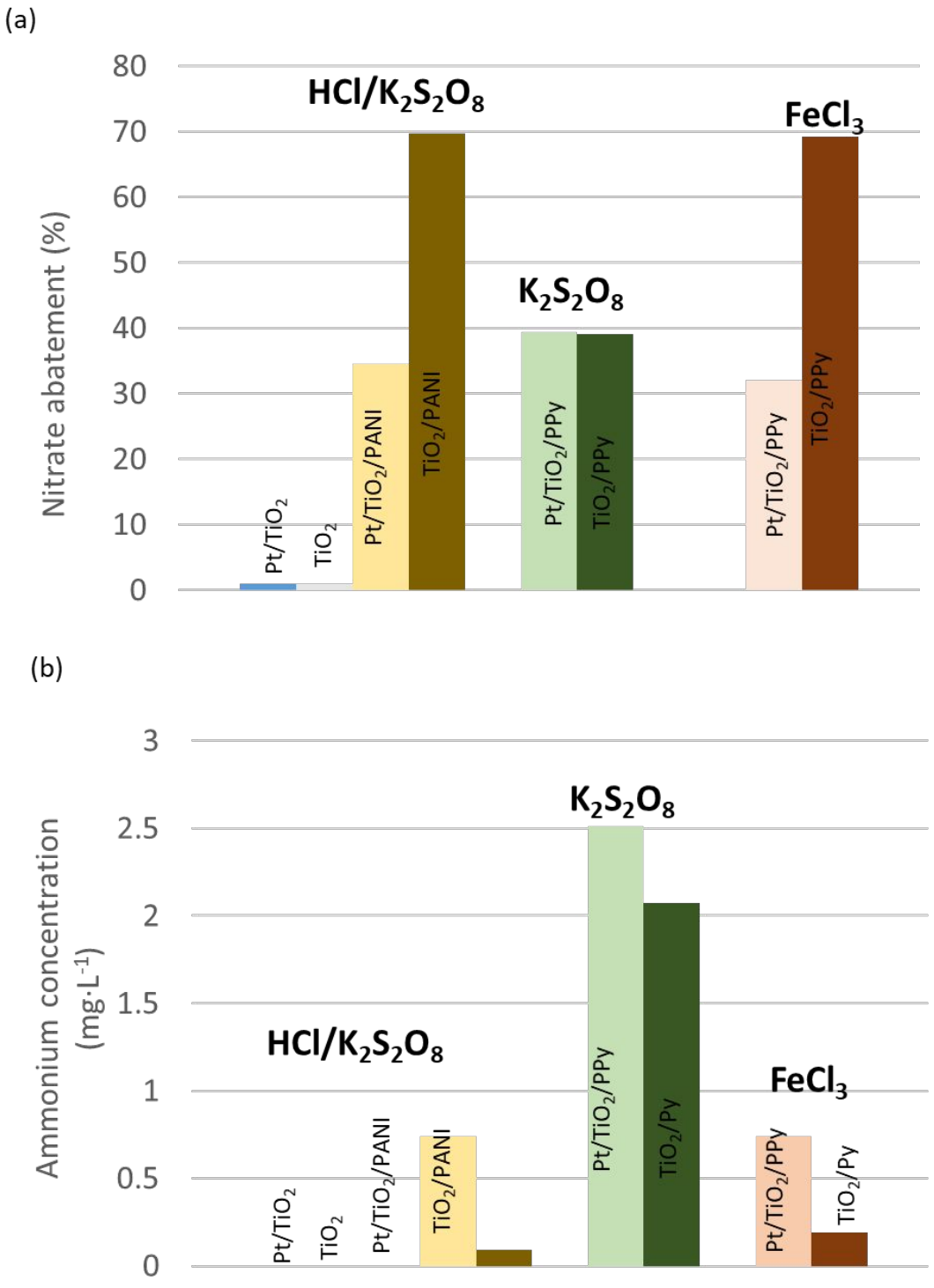


**Figure 9.** (a) Nitrate abatement and (b) ammonium concentration measured in water in the presence of the different synthesized materials. Oxidant/dopant of PANI: $K_2S_2O_8$; Oxidant/dopant of PPy: $FeCl_3$ or $K_2S_2O_8$.

**Scheme 1.** Scheme showing (a) the synthesis of $TiO_2$/PANI (b) the synthesis of $TiO_2$/PPy; (c) the resulting hybrid $TiO_2$/polymer hybrid materials with the polymeric chain interconecting the $TiO_2$ nanoparticles.

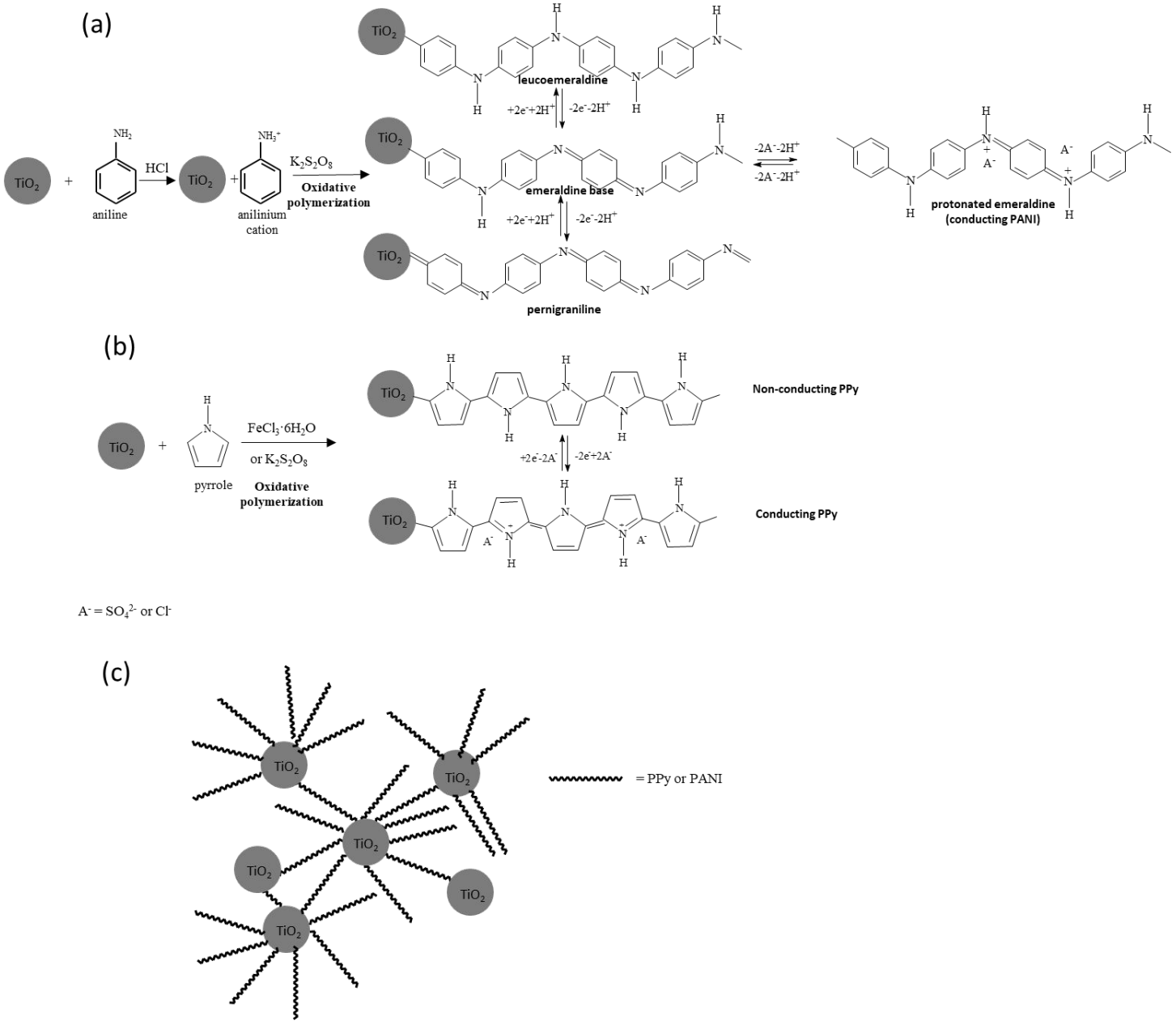

**Scheme 2.** Scheme showing (a) pyrrole chains interconecting $TiO_2$ nanoparticles; (b) nitrate exchange with the counteranion (sulfate or chloride); (c) reduction of nitrate by electrons provided by the polypyrrole.

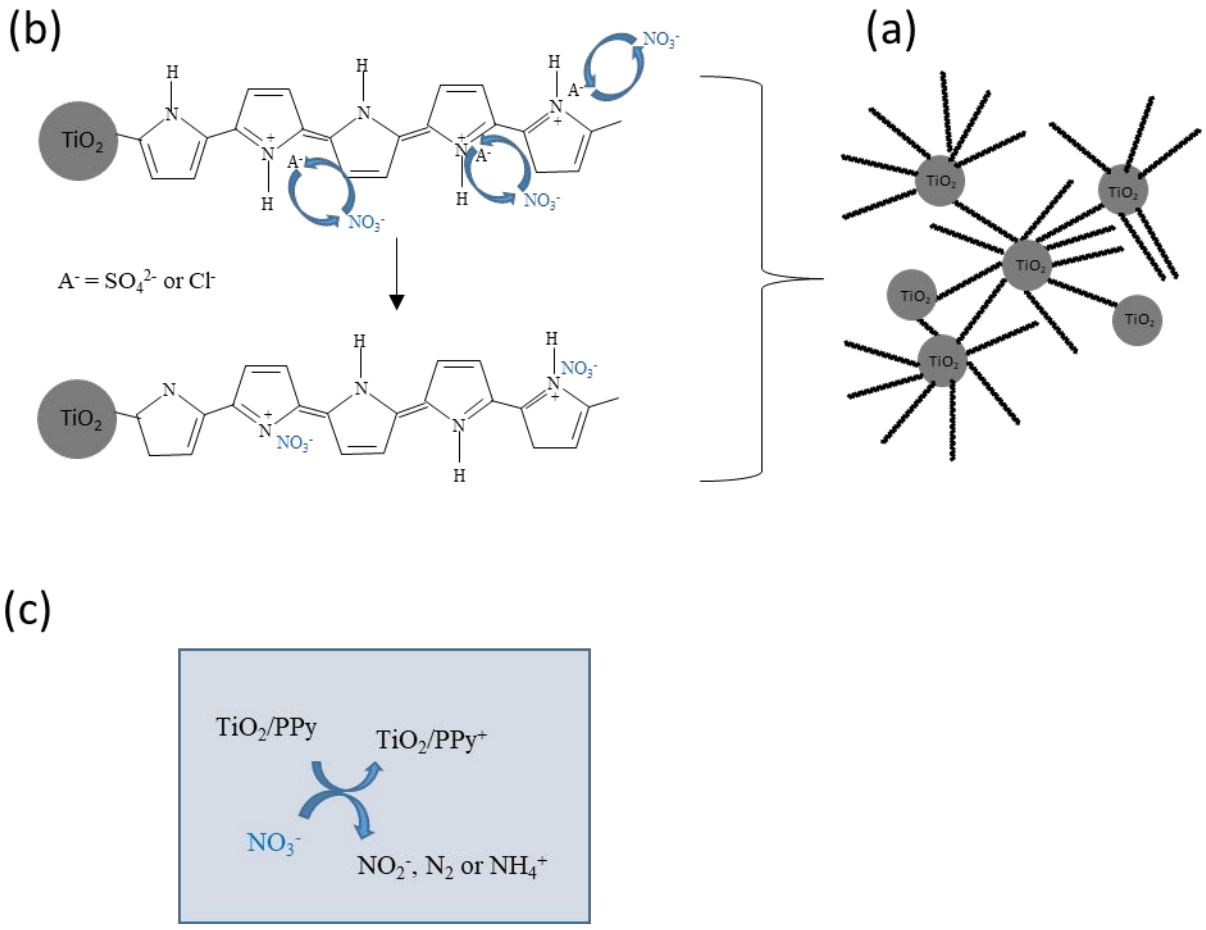

**Scheme 3.** Scheme showing (a) polypyrrole chains doped with chloride or sulfate anions interconecting $TiO_2$ nanoparticles; (b) impregnation with a platinum salt precursor producing platinum chlorocomplexes anchored to the pyrrole chain trough the pirrolic nitrogen; (c) platinum nanoparticles generated by electrons in the argon plasma; (d-e) nitrate exchange with the counteranion (sulfate or chloride); (f) reduction of nitrate by electrons provided by the polypyrrole.

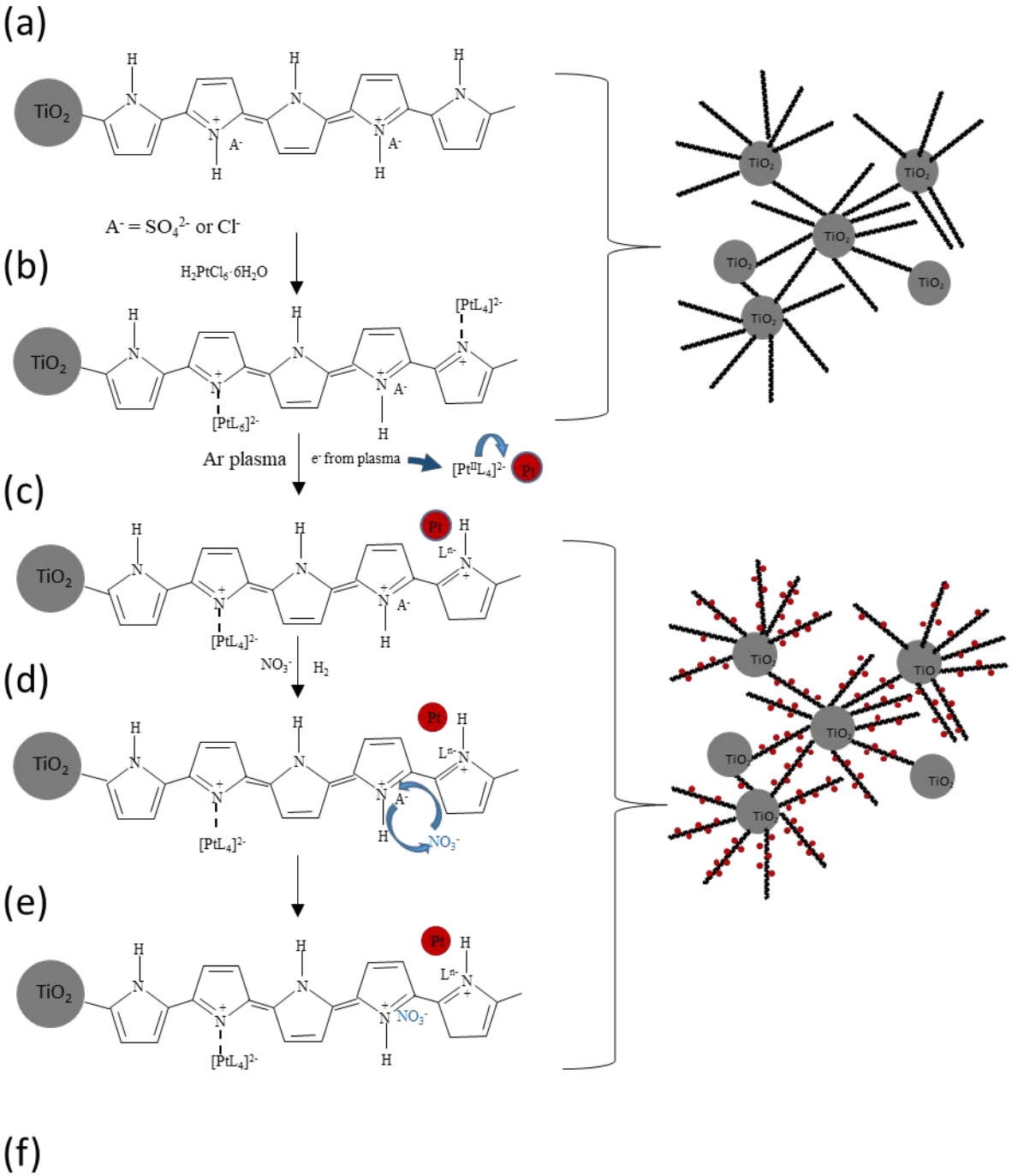

REFERENCES

1. *EC (European Community), Official Journal of the European Communities, Council Directive 98/83/EC on the Quality of Water Intended for Human Consumption, The Drinking Water Directive (DWD), Brussels, 1998, Annex 1, Part B,.*; 1998. http://www.szu.cz/uploads/documents/chzp/voda/pdf/proc99.pdf.

2. *USEPA (United State Environmental Protection Agency), National Primary Drinking Water Regulations, Washington, DC, 2008, Title 40, Part 141.*; 2008. https://www.epa.gov/sites/production/files/2015-11/documents/howepargulates_cfr-2003-title40-vol20-part141_0.pdf.

3. Shrimali M, Singh KP. New methods of nitrate removal from water. 2001;112:351-359.

4. Dodouche I, Barbosa DP, Rangel M do C, Epron F. Promoting effect of electroactive polymer supports on the catalytic performances of palladium-based catalysts for nitrite reduction in water. *Appl Catal B Environ*. 2009;76(1-2):291-299. doi:10.1016/j.apcatb.2007.06.002.

5. Al Bahri M, Calvo L, Gilarranz MA, Rodriguez JJ, Epron F. Activated carbon supported metal catalysts for reduction of nitrate in water with high selectivity towards N2. *Appl Catal B Environ*. 2013;138-139:141-148. doi:10.1016/j.apcatb.2013.02.048.

6. Soares OSGP, Órfão JJM, Ruiz-Martínez J, Silvestre-Albero J, Sepúlveda-Escribano A, Pereira MFR. Pd-Cu/AC and Pt-Cu/AC catalysts for nitrate reduction with hydrogen: Influence of calcination and reduction temperatures. *Chem Eng J*.

2010;165(1):78-88. doi:10.1016/j.cej.2010.08.065.

7. Nakamura K, Yoshida Y, Mikami I, Okuhara T. Selective hydrogenation of nitrate in water over Cu-Pd/mordenite. *Appl Catal B Environ*. 2006;65(1-2):31-36. doi:10.1016/j.apcatb.2005.12.012.

8. Garron A, Lázár K, Epron F. Effect of the support on tin distribution in Pd-Sn/Al2O 3 and Pd-Sn/SiO2 catalysts for application in water denitration. *Appl Catal B Environ*. 2005;59(1-2):57-69. doi:10.1016/j.apcatb.2005.01.002.

9. Maia MP, Rodrigues MA, Passos FB. Nitrate catalytic reduction in water using niobia supported palladium-copper catalysts. *Catal Today*. 2007;123(1-4):171-176. doi:10.1016/j.cattod.2007.01.051.

10. D'Arino M, Pinna F, Strukul G. Nitrate and nitrite hydrogenation with Pd and Pt/SnO2catalysts: The effect of the support porosity and the role of carbon dioxide in the control of selectivity. *Appl Catal B Environ*. 2004;53(3):161-168. doi:10.1016/j.apcatb.2004.05.015.

11. He D, Zeng C, Xu C, et al. Polyaniline-functionalized carbon nanotube supported platinum catalysts. *Langmuir*. 2011;27(9):5582-5588. doi:10.1021/la2003589.

12. Xu Z, Chen L, Shao Y, Yin D, Zheng S. Catalytic hydrogenation of aqueous nitrate over Pd-Cu/ZrO2 catalysts. *Ind Eng Chem Res*. 2009;48(18):8356-8363. doi:10.1021/ie9005854.

13. Epron F, Gauthard F, Pinéda C, et al. Synthesis, characterization and catalytic properties of polypyrrole-supported catalysts. *J Catal*. 2003;4(8):435-439. doi:10.1006/jcat.2000.3138.

14. Sá J, Anderson JA. FTIR study of aqueous nitrate reduction over Pd/TiO2. *Appl Catal B Environ*. 2008;77(3-4):409-417. doi:10.1016/j.apcatb.2007.08.013.

15. Zhang F, Jin R, Chen J, et al. High photocatalytic activity and selectivity for nitrogen in nitrate reduction on Ag/TiO2 catalyst with fine silver clusters. *J Catal*. 2005;232(2):424-431. doi:10.1016/j.jcat.2005.04.014.

16. Anderson JA. Photocatalytic nitrate reduction over Au / TiO 2. 2011;175:316-321. doi:10.1016/j.cattod.2011.04.009.

17. Ranjit KT, Viswanathan B. Photocatalytic reduction of nitrite and nitrate ions to ammonia on M/TiO2 catalysts. *J Photochem Photobiol A Chem*. 1997;108(1):73-78. doi:10.1016/S1010-6030(96)04505-4.

18. Sá J, Agüera CA, Gross S, Anderson JA. Photocatalytic nitrate reduction over metal modified TiO2. *Appl Catal B Environ*. 2009;85(3-4):192-200. doi:10.1016/j.apcatb.2008.07.014.

19. Barbosa DP, Tchiéta P, Rangel MDC, Epron F. The use of a cation exchange resin for palladium-tin and palladium-indium catalysts for nitrate removal in water. *J Mol Catal A Chem*. 2013;366:294-302. doi:10.1016/j.molcata.2012.10.008.

20. Martínez J, Ortiz A, Ortiz I. State-of-the-art and perspectives of the catalytic and electrocatalytic reduction of aqueous nitrates. *Appl Catal B Environ*. 2017;207:42-59. doi:10.1016/j.apcatb.2017.02.016.

21. Guo S, Heck K, Kasiraju S, et al. Insights into Nitrate Reduction over Indium-Decorated Palladium Nanoparticle Catalysts. *ACS Catal*. 2018;8(1):503-515. doi:10.1021/acscatal.7b01371.

22. Seraj S, Kunal P, Li H, Henkelman G, Humphrey SM, Werth CJ. PdAu Alloy Nanoparticle Catalysts: Effective Candidates for Nitrite Reduction in Water. *ACS Catal*. 2017;7(5):3268-3276. doi:10.1021/acscatal.6b03647.

23. Soares OSGP, Pereira MFR, Órfão JJM, Faria JL, Silva CG. Photocatalytic nitrate reduction over Pd-Cu/TiO2. *Chem Eng J*. 2014;251:123-130. doi:10.1016/j.cej.2014.04.030.

24. Barrab??s N, S?? J. Catalytic nitrate removal from water, past, present and future perspectives. *Appl Catal B Environ*. 2011;104(1-2):1-5. doi:10.1016/j.apcatb.2011.03.011.

25. Soares OSGP, Jardim EO, Reyes-Carmona ??lvaro, et al. Effect of support and pre-treatment conditions on Pt-Sn catalysts: Application to nitrate reduction in water. *J Colloid Interface Sci*. 2012;369(1):294-301. doi:10.1016/j.jcis.2011.11.059.

26. Martínez J, Ortiz A, Ortiz I. State-of-the-art and perspectives of the catalytic and electrocatalytic reduction of aqueous nitrates. *Appl Catal B Environ*. 2017;207. doi:10.1016/j.apcatb.2017.02.016.

27. Buitrago-Sierra R, García-Fernández MJJ, Pastor-Blas MMM, et al. Environmentally friendly reduction of a platinum catalyst precursor supported on polypyrrole. *Green Chem*. 2013;15(7):1981. doi:10.1039/c3gc40346g.

28. García-Fernández MJJ, Buitrago-Sierra R, Pastor-Blas MMM, Soares OSGPSGP, Pereira MFRFR, Sepúlveda-Escribano A. Green synthesis of polypyrrole-supported metal catalysts: application to nitrate removal in water. *RSC Adv*. 2015;5(41):32706-32713. doi:10.1039/C5RA03441H.

29. Ruiz-Beviá F. Assessment of the catalytic reduction of nitrates in water from an environmental point of view [2]. *J Catal*. 2004;227(2):563-565. doi:10.1016/j.jcat.2004.08.015.

30. Radoičić M, Ćirić-Marjanović G, Spasojević V, et al. Superior photocatalytic properties of carbonized PANI/TiO2nanocomposites. *Appl Catal B Environ*. 2017;213:155-166. doi:10.1016/j.apcatb.2017.05.023.

31. Janáky C, De Tacconi NR, Chanmanee W, Rajeshwar K. Bringing conjugated polymers and oxide nanoarchitectures into intimate contact: Light-induced electrodeposition of polypyrrole and polyaniline on nanoporous WO 3 or TiO 2 nanotube array. *J Phys Chem C*. 2012;116(36):19145-19155. doi:10.1021/jp305181h.

32. Rajakani P, Vedhi C. Electrocatalytic properties of polyaniline–TiO2nanocomposites. *Int J Ind Chem*. 2015;6(4):247-259. doi:10.1007/s40090-015-0046-8.

33. Arora R, Mandal UK, Sharma P, Srivastav A. TiO2and PVA Based Polyaniline Composite Materials-A Review. *Mater Today Proc*. 2015;2(4-5):2767-2775. doi:10.1016/j.matpr.2015.07.271.

34. Han Y-G, Kusunose T, Sekino T. The preparation and characterization of organic solvent dispersible polyaniline coated titania hybrid nanocomposites. *Mater Sci Forum*. 2008;569:161-164. doi:10.4028/0-87849-472-3.161.

35. Dong H, Zeng G, Tang L, et al. An overview on limitations of TiO<inf>2</inf>-based particles for photocatalytic degradation of organic pollutants and the

corresponding countermeasures. *Water Res*. 2015;79:128-146. doi:10.1016/j.watres.2015.04.038.

36. Sangareswari M, Meenakshi Sundaram M. Development of efficiency improved polymer-modified TiO2 for the photocatalytic degradation of an organic dye from wastewater environment. *Appl Water Sci*. 2017;7(4):1781-1790. doi:10.1007/s13201-015-0351-6.

37. Arora R, Srivastav A, Mandal UK. Polyaniline Based Polymeric Nano composite Containing TiO2 and SnO 2 for Environmental and Energy Applications. *Int J Mod Eng Res*. 2012;2(4):2384-2395.

38. Radoičić M, Šaponjić Z, Janković IA, Ćirić-Marjanović G, Ahrenkiel SP, Čomor MI. Improvements to the photocatalytic efficiency of polyaniline modified TiO2 nanoparticles. *Appl Catal B Environ*. 2013;136-137:133-139. doi:10.1016/j.apcatb.2013.01.007.

39. Nowotny MK, Bogdanoff P, Dittrich T, Fiechter S, Fujishima A, Tributsch H. Observations of p-type semiconductivity in titanium dioxide at room temperature. *Mater Lett*. 2010;64(8):928-930. doi:10.1016/j.matlet.2010.01.061.

40. Das S, Liu D, Park JB, Hahn YB. Metal-ion doped p-type TiO2 thin films and their applications for heterojunction devices. *J Alloys Compd*. 2013;553(3):188-193. doi:10.1016/j.jallcom.2012.11.110.

41. Li Q, Wang X, Jin Z, et al. n/p-Type changeable semiconductor TiO2 prepared from NTA. *J Nanoparticle Res*. 2007;9(5):951-957. doi:10.1007/s11051-006-9095-4.

42. Martinez U, Hammer B. Adsorption properties versus oxidation states of rutile TiO

2(110). *J Chem Phys*. 2011;134(19). doi:10.1063/1.3589861.

43. Salaoru I, Prodromakis T, Khiat A, et al. Resistive switching of oxygen enhanced TiO2 thin-film devices Resistive switching of oxygen enhanced TiO 2 thin-film devices. 2016;013506(May):1-5. doi:10.1063/1.4774089.

44. Anitha VC, Banerjee AN, Joo SW. Recent developments in TiO2 as n- and p-type transparent semiconductors: synthesis, modification, properties, and energy-related applications. *J Mater Sci*. 2015;50(23):7495-7536. doi:10.1007/s10853-015-9303-7.

45. García-Fernández MJJ, Sancho-Querol S, Pastor-Blas MMM, Sepúlveda-Escribano A. Surfactant-assisted synthesis of conducting polymers. Application to the removal of nitrates from water. *J Colloid Interface Sci*. 2017;494:98-106. doi:10.1016/j.jcis.2017.01.081.

46. T.A. Skotheim, J.R. Reynolds E. *Handbook of Conducting Polymers, Conjugated Polymers, Theory, Synthesis, Properties and Characterization*.; 2007.

47. Ohtani B, Prieto-Mahaney OO, Li D, Abe R. What is Degussa (Evonic) P25? Crystalline composition analysis, reconstruction from isolated pure particles and photocatalytic activity test. *J Photochem Photobiol A Chem*. 2010;216(2-3):179-182. doi:10.1016/j.jphotochem.2010.07.024.

48. Dodouche I, Epron F. Promoting effect of electroactive polymer supports on the catalytic performances of palladium-based catalysts for nitrite reduction in water. *Appl Catal B Environ*. 2007;76(3-4):291-299. doi:10.1016/j.apcatb.2007.06.002.

49. Stejskal J, Gilbert RG. POLYANILINE. PREPARATION OF A CONDUCTING POLYMER (IUPAC Technical Report). *Pure Appl ChemRussia J Janca (France); N*

*Gospod (France); M Helmstedt (Germany); I Krivka (Czech Republic); P Mokreva (Bulgaria J Prokes (Czech Republic); A Riede (Germany); E Rozova (Russia); I Sapurina (Russia); T Shishkanova (France);*. 2002;74(5):857867. doi:10.1351/pac200274050857.

50. Silva CHB, Da Costa Ferreira AM, Constantino VRL, Temperini MLA. Hybrid materials of polyaniline and acidic hexaniobate nanoscrolls: high polaron formation and improved thermal properties. *J Mater Chem A*. 2014;2(22):8205-8214. doi:10.1039/C4TA00737A.

51. Hasik M, Bernasik A, Adamczyk A, Malata G, Kowalski K, Camra J. Polypyrrole-palladium systems prepared in PdCl2 aqueous solutions. *Eur Polym J*. 2003;39(8):1669-1678. doi:10.1016/S0014-3057(03)00053-3.

52. Ouyang J, Li Y. Great improvement of polypyrrole films prepared electrochemically from aqueous solutions by adding nonaphenol polyethyleneoxy (10) ether. *Polymer (Guildf)*. 1997;38(15):3997-3999.

53. Nyczyk A, Sniechota A, Adamczyk A, Bernasik A, Turek W, Hasik M. Investigations of polyaniline-platinum composites prepared by sodium borohydride reduction. *Eur Polym J*. 2008;44(6):1594-1602. doi:10.1016/j.eurpolymj.2008.03.004.

54. Ohtani B, Ogawa Y, Nishimoto S. Photocatalytic Activity of Amorphous-Anatase Mixture of Titanium ( IV ) Oxide Particles Suspended in Aqueous Solutions. *J Phys Chem B*. 1997;5647(Iv):3746-3752. doi:10.1021/jp962702+.

55. Viswanathan B, Raj KJA. Effect of surface area, pore volume and particle size of

P25 titania on the phase transformation of anatase to rutile. *Indian J Chem - Sect A Inorganic, Phys Theor Anal Chem*. 2009;48(10):1378-1382.

56. Mahendra Kumar S, Deshpande PA, Krishna M, Krupashankara MS, Madras G. Photocatalytic activity of microwave plasma-synthesized tio 2 nanopowder. *Plasma Chem Plasma Process*. 2010;30(4):461-470. doi:10.1007/s11090-010-9235-6.

57. Drelinkiewicz A, Zięba A, Sobczak JW, et al. Polyaniline stabilized highly dispersed Pt nanoparticles: Preparation, characterization and catalytic properties. *React Funct Polym*. 2009;69(8):630-642. doi:10.1016/j.reactfunctpolym.2009.04.007.

58. Katoch A, Burkhart M, Hwang T, Kim SS. Synthesis of polyaniline/TiO2 hybrid nanoplates via a sol-gel chemical method. *Chem Eng J*. 2012;192:262-268. doi:10.1016/j.cej.2012.04.004.

59. Li X, Wang D, Cheng G, Luo Q, An J, Wang Y. Preparation of polyaniline-modified TiO2 nanoparticles and their photocatalytic activity under visible light illumination. *Appl Catal B Environ*. 2008;81(3-4):267-273. doi:10.1016/j.apcatb.2007.12.022.

60. Simonsen ME, Jensen H, Li Z, Søgaard EG. Surface properties and photocatalytic activity of nanocrystalline titania films. *J Photochem Photobiol A Chem*. 2008;200(2-3):192-200. doi:10.1016/j.jphotochem.2008.07.013.

61. Yu J, Zhao X, Zhao Q. Effect of surface structure on photocatalytic activity of TiO2 thin films prepared by sol-gel method. *Thin Solid Films*. 2000;379(1-2):7-14. doi:10.1016/S0040-6090(00)01542-X.

62. Tyagi S, Rawtani D, Khatri N, Tharmavaram M. Strategies for Nitrate removal from aqueous environment using Nanotechnology: A Review. *J Water Process Eng*.

2018;21(September 2017):84-95. doi:10.1016/j.jwpe.2017.12.005.

63. Kitamura Y, Niwa T, Naya S, Hattori T, Sumida Y, Tada H. In situ room temperature synthesis of a polyaniline–gold–titanium( <scp>iv</scp> ) dioxide heteronanojunction system. *Chem Commun*. 2013;49(5):520-522. doi:10.1039/C2CC37172C.

64. Dimitrijevic NM, Tepavcevic S, Liu Y, Rajh T, Silver SC, Tiede DM. Nanostructured TiO 2 / Polypyrrole for Visible Light Photocatalysis. *J Phys Chem C*. 2013;117(30):15540-15544. doi:10.1021/jp405562b.

65. Li Y, Yu Y, Wu L, Zhi J. Processable polyaniline/titania nanocomposites with good photocatalytic and conductivity properties prepared via peroxo-titanium complex catalyzed emulsion polymerization approach. *Appl Surf Sci*. 2013;273:135-143. doi:10.1016/j.apsusc.2013.01.213.

66. Deivanayaki S, Ponnuswamy V, Ashokan S, Jayamurugan P, Mariappan R. Synthesis and characterization of TiO2-doped Polyaniline nanocomposites by chemical oxidation method. *Mater Sci Semicond Process*. 2013;16(2):554-559. doi:10.1016/j.mssp.2012.07.004.

67. García-Fernández MJ, Pastor-Blas MM, Epron F, Sepúlveda-Escribano A. Proposed mechanisms for the removal of nitrate from water by platinum catalysts supported on polyaniline and polypyrrole. *Appl Catal B Environ*. 2018;225(November 2017):162-171. doi:10.1016/j.apcatb.2017.11.064.

68. Mark Weller, Tina Overton, Jonathan Rourke and FA. *Inorganic Chemistry*. 7th ed. Oxford university Press; 2018. https://global.oup.com/ukhe/product/inorganic-

chemistry-9780198768128?cc=es&lang=en&.

69. Prüsse U, Hähnlein M, Daum J, Vorlop K-D. Improving the catalytic nitrate reduction. *Catal Today*. 2000;55(2):79-90. doi:10.1016/S0920-5861(99)00228-X.

70. Prüsse U, Vorlop KD. Supported bimetallic palladium catalysts for water-phase nitrate reduction. *J Mol Catal A Chem*. 2001;173(1-2):313-328. doi:10.1016/S1381-1169(01)00156-X.

71. Mikami I, Sakamoto Y, Yoshinaga Y, Okuhara T. Kinetic and adsorption studies on the hydrogenation of nitrate and nitrite in water using Pd-Cu on active carbon support. *Appl Catal B Environ*. 2003;44(1):79-86. doi:10.1016/S0926-3373(03)00021-3.

72. Challagulla S, Tarafder K, Ganesan R, Roy S. All that Glitters Is Not Gold: A Probe into Photocatalytic Nitrate Reduction Mechanism over Noble Metal Doped and Undoped TiO2. *J Phys Chem C*. 2017;121(49):27406-27416. doi:10.1021/acs.jpcc.7b07973.

## ASSOCIATED CONTENT

Supporting information is available free of charge.

## AUTHOR INFORMATION

*Corresponding author:

E-mail: mercedes.pastor@ua.es Fax: +34-965903454; Tel: +34-965903400

## ACKNOLEWDGEMENTS

Financial support from Generalitat Valenciana, Spain (PROMETEOII/2014/004) and Ministry of Economy and Competitivity (MAT2016-80285-P) is gratefully acknowledged.

E.S. acknowledges the Spanish MINECO and AEI/FEDER (ref. CTQ2015-74494-JIN) and the University of Alicante (ref. UATALENTO16-03).

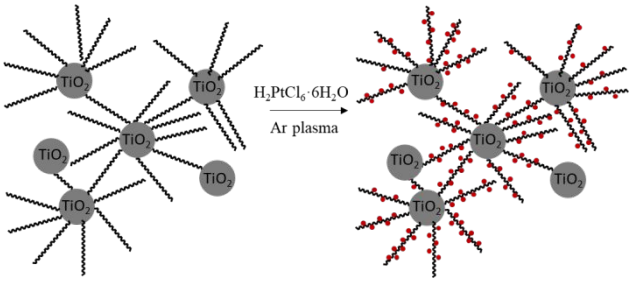


TABLE OF CONTENTS